Polariton condensation: A Green's Function approach

Jonathan Keeling

MathNanoSci Intensive Programme, L'Aquila 2010.

Contents

Contents **iii**

List of Figures **iv**

Introduction **v**
Books and Review articles vi
Acknowledgements vi

1 Introduction to condensation and polaritons **1**
1.1 Condensation of a Bose gas 1
1.2 Excitons and polaritons 7

2 Polariton models and MFT **15**
2.1 Models of polariton condensates 15
2.2 Mean-field theory of polariton Dicke model 19

3 Fluctuations in the equilibrium theory **21**
3.1 Fluctuations via Green's functions 21
3.2 Green's functions for the polariton Dicke model 24

4 Non-equilibrium model and diagram technique. **31**
4.1 The model 31
4.2 Outline of mean-field theory 32
4.3 Non-equilibrium Green's functions 33
4.4 Application to polariton Dicke model 36

5 Properties of the non-equilibrium mean field theory **39**
5.1 Comparison to equilibrium result 40
5.2 High temperature limit and laser theory 41
5.3 Generic behaviour away from extremes 43

6 Fluctuations in the non-equilibrium theory **45**
6.1 Self energies and inverse photon Green's function 45
6.2 Discussion of non-condensed spectrum 48

Bibliography **55**

List of Figures

1.1 Schematic electronic spectrum & coupled quantum wells 7
1.2 Schematic semiconductor microcavity 11
1.3 Schematic polariton spectrum 12

2.1 Disorder localised exciton states 18

3.1 Diagrammatic expansion of photon Green's functions 25
3.2 Normal and anomalous self energies 26
3.3 Spectrum of normal modes in the condensed system 28
3.4 Spectral weight of for broadened case 29

4.1 Cartoon of system coupled to pumping and decay baths. 31
4.2 Keldysh time path contour. 34

5.1 Occupation of pumping baths 40
5.2 Critical temperature vs density 43
5.3 Critical κ, γ for clean system. 44
5.4 Critical κ, γ for disordered system. 44

6.1 Inverse Green's functions and spectral weight 50
6.2 Distribution set by competition of baths 51
6.3 Zeros of $\Re, \Im \left[(D^R)^{-1}\right]$ from diagrammatic approach. 53
6.4 Zeros of $\Re, \Im \left[(D^R)^{-1}\right]$ from Maxwell-Bloch equations. 54

Introduction

These lectures discuss the use of Green's functions in understanding condensation in non-equilibrium systems. The lectures thus have two aims, conceptual and technical.

The conceptual aim of these lectures is to introduce the idea of quantum condensation in general, and of condensation of quasiparticles in semiconductors in particular. The quasiparticles that will be studied in detail are exciton-polaritons; but some historic overview including exciton condensation will also be provided. Excitons are bound electron hole pairs in semiconductors, and exciton-polaritons are superpositions of excitons and photons (resulting from repeated interconversion of photons to excitons and vice versa). These quasiparticle condensates are of interest for several reasons: firstly, their light effective mass potentially allows condensation at high temperatures, up to room temperature; secondly, particularly for polaritons, they are non-equilibrium, and thus provide a bridge to lasing. As such, one conceptual aim of these lectures is to show the link between lasing and condensation illustrated for polaritons. I will also try to highlight the similarity between different kinds of quantum condensates, particularly discussing the relation between the theory used here for polariton condensates to the theory of a weakly interacting dilute Bose gas (WIDBG).

As well as the conceptual aims, these lectures also illustrate an application of Green's function approaches to condensates. There are thus also technical aims as follows: firstly, to show how Green's functions may be used to determine the fluctuation spectrum, and physical response functions (such as luminescence intensity) of a multi-component condensate; secondly to introduce non-equilibrium Green's functions as a way to discuss systems driven out of equilibrium, and to show how these reduce to simpler descriptions in various limits.

These lectures will assume some familiarity with second quantised notation, and do not provide a complete overview of Green's functions (for which, see one of the references listed below). However, they will provide a brief summary, intended to act either as a reminder for those already familiar, or as an enumeration of the important results required for those unfamiliar.

The lectures divide into a shorter first section, discussing fluctuations in an equilibrium system, and a longer second section discussing the non-equilibrium system. The aims in both are to introduce the apparatus (Green's functions, non-equilibrium approaches) that are required to address the problem, while simultaneously discussing the results that can be

derived from these approaches.

Books and Review articles

The physical content of these lectures, as applied to the polariton system is discussed primarily in two research articles: Keeling et al. [1], Szymańska et al. [2], and many of the results are discussed in the review article [3]. The non-equilibrium Green's function approach is also reviewed in a book chapter [4], which is based closely on a previous version of these lectures.

The first chapter will set the subject of polariton condensation in context by very briefly reviewing the idea of Bose condensation, condensation of a weakly interacting Bose gas, and the idea of exciton condensation. Several good books exist that review Bose condensation, for example [5]. Regarding exciton condensation, introductions can be found in some of the articles in the collection [6], or in a review [7].

Concerning general introductions to Green's functions techniques for many body systems, this is discussed in many texts on condensed matter field theory. The approach used here is perhaps closest to Abrikosov et al. [8]. This book provides a comprehensive discussion of both the derivation of Green's function techniques, and of the analytic properties, leading to the relation of temperature vs retarded and advanced Green's functions.

For the non-equilibrium Green's function technique, there are a number of possible references;

Keldysh [9] This relatively brief article is the classic reference on this subject, discussing the Keldysh time contour, the Green's function equations, and the derivation of the Boltzmann equation from the Dyson equation.

Lifshitz and Pitaevskii [10] This textbook includes a summary of a similar list of topics as the above article.

Kamenev [11] This review article addresses non-equilibrium Green's function in terms of path integrals. Such an approach has perhaps a greater overhead in setting up the formalism, but then often considerably simplifies subsequent calculations. Although this approach is not discussed in these lectures, it is the approach used in Szymańska et al. [2].

When comparing the non-equilibrium polariton condensate to laser theory, quantum optics textbooks such as Scully and Zubairy [12] may be helpful.

Acknowledgements

These lectures are based on a course previously jointly delivered with Peter Littlewood. The recent work discussed in these lectures results from collaboration with Paul Eastham, Peter Littlewood, Francesca Marchetti and Marzena Szymańska.

Chapter 1

Introduction to condensation and polaritons

This section of notes provides an introduction to condensation in general, and to condensation of excitons and polaritons in particular. In order to provide a general framework, we will first discuss condensation of a gas of weakly interacting Bosons; such a model is certainly appropriate to describe experiments on cold dilute atomic gases, and can be appropriate to a description of polaritons at low enough densities. However, to understand polariton condensation across a range of densities, we will in the next chapter introduce a somewhat less standard model of polariton condensates which takes into account saturation of excitons at high densities.

1.1 Condensation of a Bose gas

The basic idea of condensation refers to the macroscopic occupation of a single quantum mechanical mode. A straightforward conversion of this statement into an explicit formula is the requirement that the one particle density matrix:

$$\rho(r,r') = \langle \psi^\dagger(r)\psi(r')\rangle = \sum_j n_j \phi_j^*(r)\phi_j(r') \tag{1.1}$$

should have at least one eigenvalue, n_j which scales as the number of particles in the system[13] (where normalisation $\int d\mathbf{r}|\phi|^2 = 1$ is assumed). i.e. for N particles, such that $\mathrm{Tr}(\rho) = N$, one requires $\lim_{N\to\infty} n_j/N$ to be finite. This criterion means that there is a macroscopic number of particles in a single mode. In the case of a translationally invariant system, the single particle wavefunctions $\phi_j(r)$ should take the form of plane waves $\phi_j(r) = \exp(i\mathbf{k}\cdot\mathbf{r})/\sqrt{V}$, and so the existence of a macroscopic eigenvalue means that

$$\lim_{|r-r'|\to\infty} \rho(r,r') = \frac{N}{V}$$

will be finite. This latter criterion is referred to as off diagonal long range order.

Non-interacting Bose gas

The simplest example in which such behaviour is seen is a gas of non-interacting bosons in three dimensions. From the statistical mechanics of a Bose gas, the number of particles in a volume V is given by:

$$N = \frac{V}{(2\pi)^3}\int d^3k n_B(\epsilon_k) = V\frac{m^{3/2}}{\sqrt{2}\pi^2\hbar^3}\int_0^\infty d\epsilon n_B(\epsilon)\sqrt{\epsilon}d\epsilon \tag{1.2}$$

Using the form of the Bose distribution, and writing $z = e^{\beta\mu}$, this can be rewritten as:

$$n = \frac{N}{V} = \frac{(mk_BT)^{3/2}}{\sqrt{2}\pi^2\hbar^3}\frac{\sqrt{\pi}}{2}I_{3/2}(z), \qquad I_p(z) = \frac{1}{\Gamma(p)}\int_0^\infty dx\frac{zx^{p-1}}{e^x - z}dx. \tag{1.3}$$

If $\mu \to 0, z \to 1$, then the occupation of the lowest energy state will diverge; in this limit there is a macroscopic eigenvalue of the density matrix, corresponding to the $k = 0$ eigenstate. One may show that $I_{3/2}(1) = 2.612$, and so this macroscopic occupation arises at a non-zero temperature:

$$T_{\mathrm{BEC}} = \frac{2\pi\hbar^2}{mk_B}\left(\frac{n}{2.612}\right)^2. \tag{1.4}$$

While the non-interacting gas shows condensation, the behaviour of the interacting gas is more interesting, as it is only in this case that one sees features such as superfluidity (arising from the modified excitation spectrum). Furthermore, interactions are crucial in resolving what happens when there are two almost degenerate single particle states. Therefore, we turn next to the weakly interacting Bose gas.

Weakly interacting dilute Bose gas

The WIDBG model can be written as:

$$H - \mu N = \sum_k(\epsilon_k - \mu)\psi_k^\dagger\psi_k + \sum_{k,k',q}\frac{U}{2V}\psi_{k+q}^\dagger\psi_{k'-q}^\dagger\psi_{k'}\psi_k \tag{1.5}$$

$$= \int d^3r\left[\psi^\dagger\left(-\frac{\hbar^2\nabla^2}{2m} - \mu\right)\psi + \frac{U}{2}\psi^\dagger\psi^\dagger\psi\psi\right] \tag{1.6}$$

where $\psi(r) = \sum_k \psi_k e^{i\mathbf{k}\cdot\mathbf{r}}/\sqrt{V}$.

In the interacting case, we may start to describe the phase transition to a condensed state somewhat differently, by considering the conditions required in order that a condensed state should be the state that minimises the free energy of the system. If we consider a state in which all N particles are in the same single particle wavefunction $\phi(r)$, then the free energy of this state, arising from the above Hamiltonian, is of the form:

$$F = N\int d^3r\left[\frac{\hbar^2}{2m}|\nabla\phi|^2 - \mu|\phi|^2 + \frac{U(N-1)}{2}|\phi|^4\right]. \tag{1.7}$$

Minimising this with respect to ϕ leads to a self consistent equation for the single particle wavefunction ϕ, taking into account the interactions between

particles. It is convenient to rescale $\Psi(r) = \phi(r)\sqrt{N}$. Minimising, this then gives the equation:

$$\mu\Psi(r) = \left[-\frac{\hbar^2\nabla^2}{2m} + U|\Psi(r)|^2\right]\Psi(r). \tag{1.8}$$

Since there is nothing to break spatial translation symmetry, one expects that the ground state should be uniform, and by normalisation, $\Psi = \sqrt{N/V}$, so the above equation becomes $\mu = UN/V$. This approach does not provide a critical temperature; this is because the critical temperature arises from the occupation of higher excited states depopulating the condensate. Exactly this effect will be discussed in the next section in terms of fluctuations.

The argument so far has found the state that minimises energy; it is of interest to see what the energy difference is to other possible nearby states. In particular, the state we have considered can be written as:

$$|\Psi\rangle = \left(\int d^2r\phi_0(r)\hat{\psi}(r)\right)^N |\Omega\rangle = \left(\hat{\psi}_0\right)^N |\Omega\rangle. \tag{1.9}$$

If we suppose there are two closely separated states, ϕ_0 and ϕ_1, the we may compare the energy difference between the above state and:

$$|\Psi\rangle = \left(\hat{\psi}_0\right)^{N-M}\left(\hat{\psi}_1\right)^M |\Omega\rangle. \tag{1.10}$$

The energy difference has two contributions, the kinetic energy difference is $N\Delta\epsilon$, where $\Delta\epsilon$ is the difference of single particle kinetic energies. The interaction energy difference is given by:

$$\begin{aligned}\frac{U}{2V}\left[(N-M)(N-M-1) + M(M-1) + 4(N-M)M\right] \\ \simeq \frac{U}{2V}\left[N^2 + 2M(N-M)\right].\end{aligned} \tag{1.11}$$

Noting the factors of V, and the fact that the kinetic energy difference between two low lying states scales as $\Delta\epsilon \propto V^{-2/3}$, it is clear that the dominant energy cost comes from the interactions, and that it favours a non-fragmented state, with $M = 0$ or $M = N$.

Even when considering a single, non-fragmented state, there remains more than one possible state with almost degenerate energy, and the same average number of particles. In terms of the single particle state creation operator $\psi_0^\dagger$, the two states of interest are:

$$|\Psi_N\rangle = \left(\hat{\psi}_0\right)^N |\Omega\rangle, \qquad |\Psi_\lambda\rangle = e^{\lambda\psi_0^\dagger - |\lambda|^2/2}|\Omega\rangle. \tag{1.12}$$

The second state has an indeterminate number of particles, but an average number of $|\lambda|^2 = N$. There is a small energy difference between these two states, but nothing that is extensively smaller. However, by considering fluctuations, as discussed below, there are reasons to favour this coherent state. The idea of a state with an indeterminate number of particles may be

disturbing, but there are a number of explanations. Firstly, in order that a state should be able to show interference effects, it must have a sufficiently well defined phase, and since phase and number are conjugate, thus an indefinite number of particles is necessary to show coherent interference. Secondly, when we consider fluctuations below, it will be seen that one can find states with fixed total numbers of particles, but indeterminate division of particles between the $k = 0$ mode and non-zero k modes and these states arise by considering fluctuations on top of the coherent state.

Fluctuations

We next consider the effective Hamiltonian for fluctuations on top of the macroscopically occupied state. This has several purposes: it allows one to find the excitation spectrum, which controls how the condensate responds to certain probes; it allows one to understand the depletion of condensate density at finite temperature, as excitations are populated instead of the ground state; and it also allows one to improve upon the ground state ansatz assumed above, in which all particles are in the same state.

Working in momentum space, we will consider fluctuations on top of the coherent state $|\Psi\rangle = \exp(\lambda\psi_0^\dagger)|\Omega\rangle$, where $\lambda = \sqrt{N} = \sqrt{V\mu/U}$ as discussed above. This means one may replace the operator ψ_k by $\psi_k \to \lambda\delta_k + \delta\psi_k$, in terms of the finite momentum fluctuations ψ_k. Substituting this into the WIDBG Hamiltonian then yields:

$$H_{\text{fluct}} = \sum_k (\epsilon_k - \mu)\psi_k^\dagger\psi_k + \frac{U}{2}\frac{\lambda^2}{V}\left(4\psi_k^\dagger\psi_k + \psi_k^\dagger\psi_{-k}^\dagger + \psi_k\psi_{-k}\right), \quad (1.13)$$

where we have used $H \to H = H - \mu N$, and assumed that ψ_0 is real. Then, substituting the value of λ^2, we get:

$$H_{\text{fluct}} = \sum_k (\epsilon_k + \mu)\psi_k^\dagger\psi_k + \frac{\mu}{2}\left(\psi_k^\dagger\psi_{-k}^\dagger + \psi_k\psi_{-k}\right) \quad (1.14)$$

$$= \sum_k \frac{1}{2}\begin{pmatrix}\psi_k^\dagger & \psi_{-k}\end{pmatrix}\begin{pmatrix}\epsilon_k + \mu & \mu \\ \mu & \epsilon_k + \mu\end{pmatrix}\begin{pmatrix}\psi_k \\ \psi_{-k}^\dagger\end{pmatrix} - \frac{(\epsilon_k + \mu)}{2}. \quad (1.15)$$

Here, the last line involved changing the order of two operators, so the final term comes from the commutator of $[\psi_{-k}, \psi_{-k}^\dagger]$. One now uses a Bogoliubov transformation to diagonalise the matrix, noting that since this will mix $\psi_{-k}^\dagger$ and ψ_k, it is not a unitary transformation, but rather:

$$\begin{pmatrix}\psi_k \\ \psi_{-k}^\dagger\end{pmatrix} = \begin{pmatrix}\cosh(\theta) & \sinh(\theta) \\ \sinh(\theta) & \cosh(\theta)\end{pmatrix}\begin{pmatrix}\phi_k \\ \phi_{-k}^\dagger\end{pmatrix} \quad (1.16)$$

after which the matrix in the Hamiltonian becomes:

$$\begin{pmatrix}(\epsilon_k + \mu)\cosh(2\theta) + \mu\sinh(2\theta) & (\epsilon_k + \mu)\sinh(2\theta) + \mu\cosh(2\theta) \\ (\epsilon_k + \mu)\sinh(2\theta) + \mu\cosh(2\theta) & (\epsilon_k + \mu)\cosh(2\theta) + \mu\sinh(2\theta)\end{pmatrix} \quad (1.17)$$

Hence, taking $\sinh(2\theta) = -\mu/\xi, \cosh(2\theta) = (\epsilon+\mu)/\xi$, and $\xi^2 = (\epsilon+\mu)^2 - \mu^2 = \epsilon(\epsilon+2\mu)$, one finally gets:

$$H_{\text{fluct}} = \sum_k \xi_k \phi_k^\dagger \phi_k + \frac{\xi_k - \epsilon_k - \mu}{2} \tag{1.18}$$

From this form, we may note several points:

- The mean-field ansatz was not the ground state, since in the absence of populating the finite k modes, the energy of H_{fluct} would be zero, whereas Eq. (1.18) implies it may be smaller, since $\epsilon_k + \mu > \xi_k$.
- Regardless of the temperature[1], the energy of an excitation with momentum k is given by ξ_k, hence the spectrum of fluctuations is straightforward.
- At a finite temperature, there will be a thermal occupation of the fluctuations, hence the total occupation is $N = N_{\text{cond}} + N_{\text{fluct}}$. The population of the fluctuations N_{fluct} is given by:

$$\begin{aligned}\sum_k \langle \psi_k^\dagger \psi_k \rangle &= \sum_k \cosh^2(\theta)\langle \phi_k^\dagger \phi_k \rangle + \sinh^2(\theta)\langle \phi_{-k}\phi_{-k}^\dagger \rangle \\ &= \sum_k \frac{\epsilon_k + \mu}{\xi_k} n_B(\xi_k) + \frac{(\epsilon_k + \mu - \xi_k)}{2\xi_k}.\end{aligned} \tag{1.19}$$

Thus, with increasing temperature, for a fixed N, the value of $|\lambda|^2$ will fall. This reproduces the standard form for the critical temperature for Bose-condensation, but starting from the non-condensed side.[2]

Nature of the ground state

Let us briefly note the existence in Eq. (2.22) of a contribution that exists even at $T = 0$. This is another reflection of the statement that the empty state is not the ground state; turning this around, we may note that the ground state of the fluctuation Hamiltonian, $|\Omega\rangle$ obeys:

$$0 = \phi_k|\Omega\rangle = \left(\cosh(\theta_k)\psi_k - \sinh(\theta_k)\psi_{-k}^\dagger\right)|\Omega\rangle \tag{1.21}$$

which is satisfied by:

$$|\Omega\rangle = \prod \exp\left(\tanh(\theta_k)\psi_k^\dagger \psi_{-k}^\dagger\right)|0\rangle. \tag{1.22}$$

[1] Up to the fact that the condensate density will vary with temperature

[2] To find the total density, one may use that $N = -dF/d\mu$. Evaluating this for $H = H_0 + H_{\text{fluct}}$ gives:

$$N = |lambda|^2 - \sum_k \left(\langle \psi_k^\dagger \psi_k \rangle + \frac{\langle \psi_k \psi_{-k} \rangle + \langle \psi_k^\dagger \psi_{-k}^\dagger \rangle}{2} \right). \tag{1.20}$$

The negative sign in this is at first surprising, but can be understood as meaning that, in the presence of fluctuations, $N_{\text{cond}} = N - N_{\text{fluct}} \neq |$
$lambda|^2$, since $|$
$lambda|^2$ was only the mean field estimate of the condensate density.

This describes the effect of quantum fluctuations, modifying the ground state due to interactions. It is a simple exercise to check this reproduces the $T = 0$ population in Eq. (2.22). Furthermore, one may also note that is now possible to consider taking Eq. (1.22) and projecting it onto a fixed total number of particles; such a state then has a well defined total number, but an ill-defined number of particles in the $k = 0$ mode. This result is in part justification for the assumption above that we should consider a coherent state.

Two dimensions

The above discussion showed that in three dimensions, there can be a condensate of either non-interacting, or of interacting Bose particles. Since the systems we will be interested in are generally two dimensional (i.e. excitons are confined in planar quantum wells, and polaritons involve photons confined in microcavities), we will thus discuss briefly here the differences between condensation in two and three dimensions. For a non-interacting Bose gas in two dimensions, the equivalent of Eq. (1.3) is instead:

$$n_{\rm 2D} = \frac{N}{A} = \frac{m k_B T}{2\pi\hbar^2} I_1(z) \tag{1.23}$$

however, unlike in three dimensions, $\lim_{z\to 1} I_1(z) = \infty$, meaning that no matter what temperature or density, a non condensed solution will exist, i.e. $\mu < 0$.

The fact that a non-interacting two dimensional gas has no phase transition does not mean that an interacting system is prevented from having a phase transition. There is however a stronger statement that fluctuations will always destroy long range order for a phase transition involving breaking of a continuous symmetry in two dimensions. Since the condensation transition breaks the phase rotation symmetry (as is particularly clear for the coherent state discussed above), this does apply to a two dimensional interacting system. Yet, despite this restriction, a phase transition can and generally does exist at a non-zero temperature for an interacting two dimensional system.

The phase transition does not lead to condensation (at least in a finite system), in that there is no single macroscopically occupied mode. There is however a change to the coherence properties, such that whereas in the normal (high temperature) phase the density matrix decays exponentially [i.e. $\rho(r, r') \propto \exp(-|r - r'|/\zeta)$], the low temperature phase instead has algebraic decay, $\rho(r, r') \propto |r - r'|^{-\eta}$. Furthermore, the low temperature phase of the interacting Bose gas is superfluid, in that it shares with the interacting three dimensional condensate the properties of having different transverse and longitudinal response, or equivalently, the property that it cannot support rotation except by creating quantised vortices.

Such complications will not be fully discussed in these lectures, however they can be straightforwardly incorporated within the formalism described, as long as one takes into account the fluctuations on top of the mean field theory. In order to understand fully the effect of these fluctuations, it is

generally convenient to work in terms of density and phase fluctuations, i.e. $\psi = \sqrt{\rho + \pi}e^{i\phi}$, where ρ is the mean field density, and π, ϕ the fluctuations. In such a language, it is the contribution of phase fluctuations that destroys long range order, and leads to power law decay of correlations. Although the non-interacting gas does not show any transition, just as in the three dimensional case, the transition temperature for the weakly interacting case can be roughly estimated from the non-interacting result, such that one has $k_B T_c \simeq 2\pi\hbar^2 n/m$.

1.2 Excitons and polaritons

Because the transition temperature for a Bose gas depends inversely on its mass, it is favourable for condensation to consider particles with relatively light masses. One way to produce particles with particularly light masses is to consider quasiparticles inside semiconductors. Since a bosonic quasiparticle is required, one of the simplest quasiparticles one might consider here is the exciton, a bound pair of an electron and hole. An even lighter quasiparticle can be produced by considering a mixture of excitons and photons, i.e. exciton-polaritons. The following section will introduce excitons, exciton condensation, and microcavity exciton-polaritons.

Excitons

Excitons result from Coulomb interactions between excited electrons, and holes in a semiconductor. They require an almost filled valence band, with a small number of unoccupied states to give valence band holes, and a partly occupied conduction band. In some indirect gap semi-metals, this configuration may exist in the ground state, however we will discuss here direct band gap semiconductors, where such a situation can only be created by optical excitation, transferring electrons between the valence and conduction band (see Fig. 1.1).

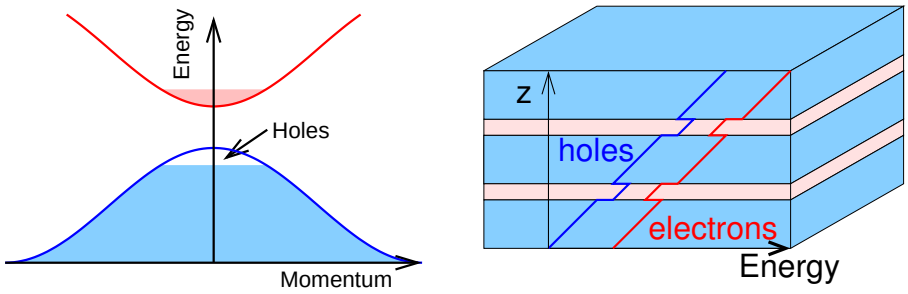

Figure 1.1: Left: Optically excited semiconductor, with an almost filled valence band, with a small number of valence band holes and conduction band electrons created. Right: Coupled quantum wells, with applied perpendicular electric field, so that electrons and holes are spatially separated into two quantum wells.

The behaviour of the system can be described in terms of a Hamiltonian

for electrons with k near the band gap:

$$H = \sum_k \left(\epsilon_c(k) a^\dagger_{ck} a_{ck} + \epsilon_v(k) a^\dagger_{vk} a_{vk} \right) + \frac{1}{2} \sum_q \left(V^{ee}_q \rho^e_q \rho^e_{-q} + V^{hh}_q \rho^h_q \rho^h_{-q} - 2V^{eh}_q \rho^e_q \rho^h_{-q} \right) \quad (1.24)$$

where $\rho^e_q = \sum_k a^\dagger_{ck+q} a_{ck}$ and $\rho^h_q = \sum_k a_{vk-q} a^\dagger_{vk}$, and the Coulomb interaction is $V(q) = e^2 4\pi/\epsilon q^2$. For small values of k, the conduction and valence band electron energies can be expanded assuming parabolic bands, $\epsilon_c(k) = \hbar^2 k^2/2m_c, \epsilon_v(k) = -E_g - \hbar^2 k^2/2|m_v|$. This Hamiltonian, written in terms of creation operators for conduction and valence band electrons can be rewritten via $h^\dagger_{-k} = a_{vk}, c_k = a_{ck}$ as a Hamiltonian for valence band holes and conduction band electrons; this has the result that the kinetic energy term then describes positive mass holes as well as positive mass conduction band electrons.

At low densities of electrons and holes, one may consider the single electron-hole pair problem, which leads to the two particle Hamiltonian:

$$H = E_g - \frac{\hbar^2 \nabla^2_e}{2m_c} - \frac{\hbar^2 \nabla^2_h}{2m_v} - \frac{e^2}{4\pi\epsilon |r_e - r_h|} \quad (1.25)$$

This has Hydrogen like solutions, parametrised by the exciton Rydberg $\mathcal{R}y_{ex} = \mu e^4/2\epsilon^2\hbar^2 = (\mu/m^*\epsilon^2)\mathcal{R}y$, and the exciton Bohr radius $a_{ex} = \epsilon\hbar^2/\mu e^2 = (\epsilon m^*/\mu)a_0$, where μ is the reduced electron-hole mass, and m^* the free electron mass. Compare to Hydrogen, the most significant effect is that $\epsilon = \epsilon_0\epsilon_r$ with $\epsilon_r \simeq 11$ for typical semiconductors; this leads to a much increased Bohr radius, and reduced binding energy. As such, it is quite feasible to approach exciton densities where excitons are separated by a distance comparable to their Bohr radius.

As one moves away from low densities, the problem of the electron-hole ground state becomes more complicated, since the high density of electronic excitation can screen the Coulomb interaction inside each exciton, leading to a possible transition to a Mott insulator phase, or some other non excitonic phase at high densities. In fact, the full phase diagram of the electron-hole system as a function of density and electron/hole mass ratio remains not fully determined.

Two further complications regarding the exciton system should be mentioned:

- The first is that the excitons can recombine, i.e. since the conduction band electrons could be formed by optical excitation, there is a non-zero probability that electrons in the conduction band can transfer back to the conduction band, emitting a photon. The rate of recombination can be calculated in terms of the light-matter coupling, which one may write as $H_{\text{int}} = -eA(R)(p_e/m_c - p_h/m_h)$, depends on the properties of the semiconductor, via the transition matrix element $\mu_{cv} = \langle ck|p/m^*|v-k\rangle$, in terms of matrix elements of the single electron states.

The lifetime also depends on the exciton wavefunction, in terms of the spatial overlap between the electron and hole. As such, the lifetime of excitons can be increased either by choosing materials with intrinsically lower dipole matrix elements, or by spatially separating electrons and holes. This can be acheived by confining electrons and holes in separate quantum wells, as illustrated in Fig. 1.1. A quantum well (QW) can be created by growing a semiconductor heterostructure, i.e. changing between two different semiconducting materials, such that the band structure — the energy of the single electron states as a function of momentum — is different in a thin layer. If this thin layer is chosen so that the energy of valence electrons is higher, and that of conduction electrons is lower, then both electrons and holes will be preferentially found inside this QW. In order to avoid dislocations in the semiconductor (which would otherwise induce disorder that can trap electrons and holes), QWs typically involve ternary alloys matched to binary alloys of the surrounding material, e.g. $Al_xGa_{1-x}As$ wells grown in $GaAs$ substrates, or $Mg_xCd_{1-x}Te$ wells in $CdTe$. By then applying a perpendicular electric field across the whole structure, one may ensure that electrons are confined in one well, while holes are confined in another well. This significantly reduces the electron hole overlap, and thus increases the lifetime.

- The other complication is that there exist parts of the Coulomb interaction that lead to the spontaneous creation of electron hole pairs; i.e. inter-band scattering via the Coulomb term:

$$\sum_{k,k',q} V_q a^\dagger_{ck+q} a^\dagger_{vk'-q} a_{vk'} a_{vk} = \sum_{k,k',q} V_q c^\dagger_{k+q} h_{q-k'} h^\dagger_{-k'} h^\dagger_{-k}. \qquad (1.26)$$

Such terms are important for exciton condensation, as even if small, they cause the phase of the excitonic condensate to lock, so that the excitation spectrum for excitons is gapped — such a term would be analogous to a term in the WIDBG model looking like $(\psi + \psi^\dagger)$.

Exciton condensation

Starting from the low density limit, just as for the weakly interacting Bose gas, one may write an approximate state for an exciton condensate in terms of a coherent state of excitons. The operator creating a single ground state exciton has the form:

$$|\Phi_0\rangle = \frac{1}{\sqrt{V}} \sum_k \phi_{1s}(k) c^\dagger_k h^\dagger_{-k} |\Omega\rangle = \frac{1}{\sqrt{V}} \sum_k \phi_{1s}(k) a^\dagger_{ck} a_{vk} |\Omega\rangle \qquad (1.27)$$

where $\phi_{1s}(k)$ is the Fourier transform of the 1s wavefunction for the Coulomb potential. The state $|\Omega\rangle$ may be described either as the vacuum for conduction electrons and valence holes, or equivalently, as the filled valence band.

This then prompts one to write the exciton condensate wavefunction as:

$$|\Psi_{\text{ex. cond.}}\rangle = \mathcal{N} \exp\left(\sum_k \lambda_k a^\dagger_{ck} a_{vk}\right)|\Omega\rangle = \prod_k \left(u_k + v_k a^\dagger_{ck} a_{vk}\right)|\Omega\rangle. \tag{1.28}$$

The second expression follows from the first by replacing the exponential of the sum by a product of exponentials, and then by noting that since $a, a^\dagger$ are Fermionic operators, the Taylor expansion of the exponential should stop after the first term. We have then introduced u_k, v_k via $\lambda_k = v_k/u_k, |u_k|^2 + |v_k|^2 = 1$, with the latter criterion ensuring normalisation.

For low densities, the form $v_k \simeq \lambda_k = \sqrt{N/V}\phi_{1s}(k)$ will apply, but as density increases, and $v_k \to 1$, the form of v_k that minimise energy will start to be modified [14]. In the very high density limit, $v_k \simeq \theta(k < k_F)$, i.e. the fermionic statistics start to play a significant role, and only near the Fermi surface does the Coulomb interaction have an effect. By minimising the energy of Eq. (1.28) with Hamiltonian (1.24), one can determine the form of u_k, v_k throughout the crossover from low to high density exciton condensates[15].

As for the mean field theory of the WIDBG, this approach is a good way to describe the ground state at zero temperature, but does not necessarily determine the transition temperature. For this, one must consider the possibility of excitations, which deplete the condensate. Unlike the WIDBG, the exciton case contains two classes of excitations that one must consider:

- Fermionic excitations, corresponding to ionising excitons, by allowing for excitations in which u_k, v_k change. It is possible to straightforwardly incorporate these in a non-zero temperature mean field theory by calculating the partition function at finite temperature corresponding to these kinds of excitations, and thus find the decrease of v_k, and the associated excitonic ordering at finite temperature. An analogous calculation for exciton-polaritons is discussed later. Such excitations are the dominant effect at high densities.

- At low densities, the dominant fluctuations instead concern bound excitons, but excited to finite momentum states. These excitations are exactly as for the WIDBG, and lead to a transition temperature that depends on the excitonic mass.

Exciton-Polaritons

Microcavity exciton polaritons are the result of strong coupling between photons confined in semiconductor microcavities, and excitons in QWs. A schematic of the semiconductor structures used to engineer microcavity exciton polaritons is shown in Fig. 1.2. The semiconductor microcavity is formed by two distributed Bragg reflectors, and QWs are then placed at the antinodes of the standing wave of light in the cavity.

At the simplest level, the strong coupling between excitons and polaritons can be understood in terms of a model of non-interacting bosonic

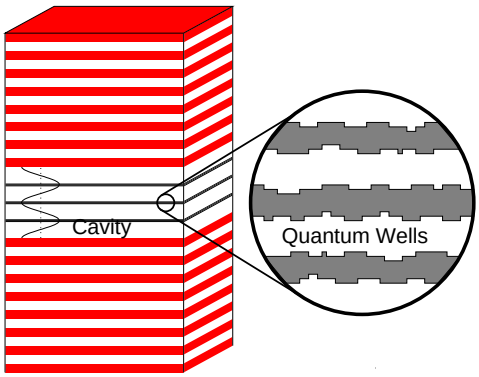

Figure 1.2: Schematic of microcavity system. Red and white alternating layers indicate layers of alternating dielectric contrast, producing a Bragg mirror. Inside the cavity between the two mirrors, quantum wells are placed at the antinodes of the standing wave pattern of light.

modes, $\psi_k^\dagger$ creating photons, $D_k^\dagger$ creating excitons (assumed for the moment to behave as bosons, if at low enough density), where $\mathbf{k}$ labels the in plane momentum. One may then write

$$H = \begin{pmatrix} \psi_k^\dagger & D_k^\dagger \end{pmatrix} \begin{pmatrix} \omega_k & \Omega_R/2 \\ \Omega_R/2 & \epsilon_k \end{pmatrix} \begin{pmatrix} \psi_k \\ D_k \end{pmatrix} \tag{1.29}$$

Here, $\omega_{\mathbf{k}}$ is the energy of the photon mode confined in the cavity of width L_w, giving: $\omega_{\mathbf{k}} = (c/n)\sqrt{k^2 + (2\pi N/L_w)^2}$, with n is the refractive index, and N the index of the transverse mode in the cavity. For small k, the energy can be written as $\omega_{\mathbf{k}} = \omega_0 + k^2/2m$, where m is an effective photon mass $m = (n/c)(2\pi/L_w)$. In the absence of disorder, the exciton energy in the QW is $\varepsilon_{\mathbf{k}} = \varepsilon_0 + k^2/2M$, where M is the total exciton mass, and $\varepsilon_0 = E_{gap} - \mathcal{R}y_{ex}$ comes from the conduction-valence band gap E_{gap} including QW confinement and the exciton binding energy (Rydberg) $\mathcal{R}y_{ex}$. For convenience, we define the bottom of the exciton band, ε_0 as the zero of energies; and denote the detuning between exciton and photon bands as $\delta = \omega_0 - \varepsilon_0$. Finally, the off diagonal term $\Omega_R/2$ describes the exciton-photon coupling, where Ω_R is the Rabi frequency. Then, diagonalising the quadratic form in Eq. (1.29) gives the polariton spectrum:

$$E_{\mathbf{k}}^{\mathrm{LP,UP}} = \frac{1}{2}\left[\left(\delta + \frac{k^2}{2M} + \frac{k^2}{2m}\right) \mp \sqrt{\left(\delta + \frac{k^2}{2M} - \frac{k^2}{2m}\right)^2 + \Omega_R^2}\right]. \tag{1.30}$$

This spectrum is illustrated in Fig. 1.3 It is shown there both as a function of momentum k, and also as a function of angle. The angle corresponds to the angle of emission of a photon out of the cavity; since the in-plane momentum and photon frequency are both conserved as photons escape through the Bragg mirrors, one may write $(\varepsilon_0 + E_{\mathbf{k}}^{LP})\sin(\theta) = ck$, which (since typical values of k satisfy $\omega_0, \varepsilon_0 \gg ck$) can be approximated as $\omega_0 \sin(\theta) = ck$.

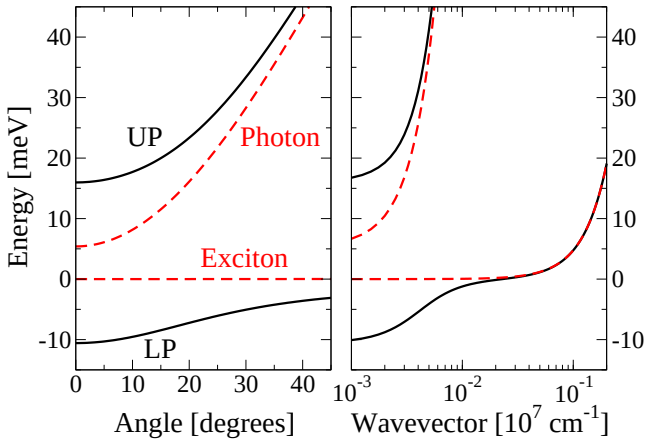

Figure 1.3: Schematic polariton spectrum: Left, plotted vs emission angle $\theta = \sin^{-1}(ck/\omega_0)$, right as a function of momentum on a logarithmic scale.

Microcavity polaritons are an interesting system in which to investigate condensation because they combine a very light effective mass (10^4 times smaller than the electron mass), with a matter component, and hence the possibility of thermalisation. These together open the possibility of polariton condensation at elevated temperatures. Polaritons however introduce another feature not normally present in, e.g., cold atomic gases. That is the finite lifetime of the quasiparticles: photons are imperfectly confined by the mirrors, and so can leak out. This means that the polariton condensate is best thought of as a steady state, balancing pumping and decay.

Table 1.1 illustrates the extent to which polaritons are out of equilibrium, compared to other examples of condensates, including cold atoms, excitons and magnetic excitations in magnetic insulators. The summary of this table is that while polaritons have a short lifetime, this is sufficiently long for them to establish a reasonably equilibrium distribution, and the ratio of lifetime to thermalisation times is not vastly different to that for other systems. On the other hand, the effect of finite lifetime on coherence is much more significant. This motivates the approach in the following chapters to understand how to describe the light emission accounting for finite lifetimes.

The next two chapters will first discuss how to model the microcavity polariton system, discussing the calculation of the mean-field theory, and of the Green's functions describing fluctuations about this mean field state. From this basis, the remainder of these lectures will study the same problem out of equilibrium.

	Lifetime	Thermalisation	Linewidth	Temperature	
Atoms	10s	10ms	2.5×10^{-13}meV	10^{-8}K	10^{-9}meV
Excitons	50ns	0.2ns	5×10^{-5}meV	1K	0.1meV
Polaritons	5ps	0.5ps	0.5meV	20K	2meV
Magnons	1μs	100ns	2.5×10^{-6}meV	300K	30meV

Table 1.1: Characteristic timescales and energies for: particle lifetimes, times to establish a thermal distribution, linewidth due to finite lifetime, and characteristic temperatures for various candidate condensates. Comparison of the first two describes how thermal the distribution will be; comparison of the later two determine the effect of finite lifetime on coherence properties.

Chapter 2

Polariton models and mean-field theory

This chapter will discuss the approach to modelling microcavity polariton systems, reviewing the approximate models that are widely used to describe these systems, and discussing the mean field theory of the model that will be discussed in the remainder of these lectures.

2.1 Models of polariton condensates

The model to describe the underlying physics of a microcavity polariton system is relatively straightforward to derive; the excitons are described by the same combination of kinetic (H_{eh}) and Coulomb interaction ($H_{\rm coul}$) terms as written previously (although now constrained to two dimensional quantum wells). The full Hamiltonian can then be written as $H = H_{\rm eh} + H_{\rm coul} + H_{\rm photon} + H_{\rm dipole} + H_{\rm disorder}$ where the additional terms describe the microcavity photons and their coupling to the excitons, and excitonic disorder. The photon term is straightforwardly given by:

$$H_{\rm photon} = \sum_{\mathbf{q}} \omega_{\mathbf{q}} \psi^\dagger_{\mathbf{q}} \psi_{\mathbf{q}} + \int d\mathbf{r} W_{\rm ph}(\mathbf{r}) \psi^\dagger(\mathbf{r}) \psi(\mathbf{r}), \tag{2.1}$$

(inlcuding possible photonic disorder). The exciton photon coupling term, i.e. the process whereby a photon is absorbed, and excites an electron from the valence band to the conduction band, thus creating an electron hole pair is described by:

$$H_{\rm dipole} = \frac{1}{\sqrt{A}} \sum_{\mathbf{q},\mathbf{k}} e\mu_{cv} \sqrt{\frac{\omega_{\mathbf{q}}}{2\epsilon_r \epsilon_0 L_w}} \left(\psi^\dagger_{\mathbf{q}} a^\dagger_{v\mathbf{k}+\mathbf{q}} a_{c\mathbf{k}} + \text{H.c.} \right) \tag{2.2}$$

In addition, we have included a term describing the effect of quantum well disorder on the excitons. This is generally more significant for polariton experiments than it would be for exciton experiments, since the characteristic density of excitons is much lower in polariton experiments[1]. Since

[1]This is possible because the polariton mass is 10^4 times smaller than the exciton mass, thus using $T_c \propto n/m$ for a two dimensional Bose gas, one can either contemplate

high exciton densities lead to all low energy states being occupied, and the disorder thus being screened, the effects of excitonic disorder are more noticeable at low densities. The disorder term can be written:

$$H_{\text{disorder}} = \int d\mathbf{r} \left[W_e(\mathbf{r}) a_c^\dagger(\mathbf{r}) a_c(\mathbf{r}) - W_h(\mathbf{r}) a_v(\mathbf{r}) a_v^\dagger(\mathbf{r}) \right] . \quad (2.3)$$

While the above Hamiltonian is reasonably comprehensive it is rather unwieldy for useful calculations; it allows for a large number of kinds of high energy excitons (such as ionising excitons etc.) that are rarely necessary in the range of temperatures and energies at which polariton condensates exist. In the following sections we will instead discuss two more approximate Hamiltonians, whose purpose is to highlight the relevant low energy excitations that determine the polariton state.

WIDBG model of polaritons

The first model is one in which bosonic operators D_k are introduced to describe the creation of a bound excitonic pair. Neglecting disorder, the quadratic part of the Hamiltonian then reduces to the previous quadratic form, describing excitons coupled to photons. However, if one expands the description to fourth order, there also then arise interaction terms between the Bosonic operators, given by:

$$\begin{aligned} H &= \sum_{\mathbf{k}} \left[\omega_{\mathbf{k}} \psi_{\mathbf{k}}^\dagger \psi_{\mathbf{k}} + \varepsilon_{\mathbf{k}} D_{\mathbf{k}}^\dagger D_{\mathbf{k}} + \frac{\Omega_R}{2} (D_{\mathbf{k}}^\dagger \psi_{\mathbf{k}} + \psi_{\mathbf{k}}^\dagger D_{\mathbf{k}}) \right] \\ &- \frac{\Omega_R}{2\rho_{sat}} \sum_{\mathbf{k},\mathbf{k}',\mathbf{q}} \left[D_{\mathbf{k}'-\mathbf{q}}^\dagger D_{\mathbf{k}+\mathbf{q}}^\dagger D_{\mathbf{k}} \psi_{\mathbf{k}'} + \psi_{\mathbf{k}'-\mathbf{q}}^\dagger D_{\mathbf{k}+\mathbf{q}}^\dagger D_{\mathbf{k}} D_{\mathbf{k}'} \right] \\ &+ \sum_{\mathbf{k},\mathbf{k}',\mathbf{q}} \frac{U_{\mathbf{k}-\mathbf{k}',\mathbf{q}}}{2} D_{\mathbf{k}+\mathbf{q}}^\dagger D_{\mathbf{k}'-\mathbf{q}}^\dagger D_{\mathbf{k}'} D_{\mathbf{k}}, \end{aligned} \quad (2.4)$$

This Hamiltonian is thus a variant on the weakly interacting dilute Bose gas model, in which there are two bosonic species, and where the interaction has a particular structure in terms of these species. The interaction terms can be described as having two parts; an exciton-exciton interaction (the last term in Eq. (2.4)), and an effective saturation term, implying that the exciton photon coupling reduces as the density increases.

This model is somewhat problematic in that it is only valid for $\sum_k D_k^\dagger D_k < \rho_{\text{sat}}$, otherwise the Hamiltonian appears to be unbounded from below. Since the ground state of the full problem generally does lie within this allowed range, it is normally possible to avoid this problem. In particular, one may project onto the lower polariton state, resulting from diagonalising the quadratic part of the Hamiltonian, using:

$$\begin{pmatrix} \psi_{\mathbf{k}}^\dagger \\ D_{\mathbf{k}}^\dagger \end{pmatrix} = \begin{pmatrix} \cos\theta_{\mathbf{k}} & -\sin\theta_{\mathbf{k}} \\ \sin\theta_{\mathbf{k}} & \cos\theta_{\mathbf{k}} \end{pmatrix} \begin{pmatrix} U_{\mathbf{k}}^\dagger \\ L_{\mathbf{k}}^\dagger \end{pmatrix} \quad (2.5)$$

increasing the transition temperature, or reducing the density compared to excitons; or as is the actual case, a compromise of both

where $U_k^\dagger, L_k^\dagger$ represent creation operators for the upper and lower polaritons. By truncating the model to the lower polariton state, one finds an effective WIDBG model, in which the previous instability problem has been eliminated.

$$H_{\rm LP} = \sum_{\mathbf{k}} E_{\mathbf{k}}^{\rm LP} L_{\mathbf{k}}^\dagger L_{\mathbf{k}} + \sum_{\mathbf{k},\mathbf{k}',\mathbf{q}} V_{\mathbf{k},\mathbf{k}',\mathbf{q}}^{\rm eff} L_{\mathbf{k}+\mathbf{q}}^\dagger L_{\mathbf{k}'-\mathbf{q}}^\dagger L_{\mathbf{k}'} L_{\mathbf{k}} \tag{2.6}$$

$$E_{\mathbf{k}}^{\rm LP} = \frac{1}{2}\left[(\omega_{\mathbf{k}} + \varepsilon_{\mathbf{k}}) - \sqrt{(\omega_{\mathbf{k}} - \varepsilon_{\mathbf{k}})^2 + \Omega_R^2}\right] \tag{2.7}$$

$$\begin{aligned} V_{\mathbf{k},\mathbf{k}',\mathbf{q}}^{\rm eff} &= \frac{\Omega_R}{2\rho_{sat}} \cos\theta_{\mathbf{k}+\mathbf{q}} \cos\theta_{\mathbf{k}} \left[\cos\theta_{\mathbf{k}'-\mathbf{q}} \sin\theta_{\mathbf{k}'} + \sin\theta_{\mathbf{k}'-\mathbf{q}} \cos\theta_{\mathbf{k}'}\right] \\ &+ \frac{U}{2} \cos\theta_{\mathbf{k}+\mathbf{q}} \cos\theta_{\mathbf{k}} \cos\theta_{\mathbf{k}'-\mathbf{q}} \cos\theta_{\mathbf{k}'} \end{aligned} \tag{2.8}$$

This Hamiltonian can be a reasonable description at low densities and in sufficiently clean (i.e. not disordered) systems, but suffers from two problems. Firstly, it does not take account of the excitonic disorder. If disorder is large, it can have an effect in changing the nature of the saturation and exciton-exciton interaction terms. However, this can be naturally incorporated by a suitable change of $V_{k,k',q}^{\rm eff}$. Secondly, when density becomes large enough that saturation effects are important, the above model is not fully able to describe the saturation: the model projected to the lower polariton band has eliminated states that may be involved at high densities, and without projection,the full Hamiltonian in Eq. (2.4) cannot be fully trusted in the case where density is comparable to $\rho_{\rm sat}$.

Localised exciton model of polaritons

In order to address the saturation effects, one may consider a rather different model, which instead starts from the assumption that disorder is strong, and so the relevant excitonic states are completely localised. In this model, one can then take account of both interaction and saturation effects by allowing each disorder site to be occupied by only zero or one exciton.

As such, this model describes a set of two-level systems, written below in terms of spin 1/2 operators $\mathbf{S}_i$, coupled to a photon field:

$$H = \sum_i 2\epsilon_i S_i^z + \sum_k \omega_k \psi_k^\dagger \psi_k + \sum_{i,k} g_i (\psi_k^\dagger S_i^- + \text{H.c.}) \tag{2.9}$$

The three terms above describe the energy of the excitons, the energy of the photons, and the process of exciton-photon interconversion. Unlike the bosonic model, this description already includes the effects of nonlinearity and saturation at this level — each two level system can only be excited once, due to the combined effects of excitation and saturation. (The factor of two in $2\epsilon_i$ is introduced purely for later convenience.)

Since the above model is based on the idea that disorder localises excitons, it is appropriate to take into account disorder when calculating the energies $2\epsilon_i$ and oscillator strengths g_i of the exciton states. This can be done by numerically diagonalising the single exciton Schrodinger equation

in the presence of a disorder potential:

$$\left[-\frac{\nabla^2_{\mathbf{R}}}{2M} + W(\mathbf{R})\right]\Phi_i(\mathbf{R}) = 2\epsilon_i\Phi_i(\mathbf{R}). \tag{2.10}$$

and then calculating the oscillator strength from

$$g_{i,\mathbf{p}} = e\mu_{cv}\sqrt{\frac{\omega_{\mathbf{p}}}{2\epsilon_r\epsilon_0 L_w}}\varphi_{1s}(0)\Phi_{i,\mathbf{p}}. \tag{2.11}$$

The exciton states found in this way are illustrated in Fig. 2.1. The principal feature of importance to take from this figure is that those states which couple most strongly to light lie at energies below the band edge of the clean system, and are thus indeed states that are significantly localised by disorder, reinforcing the idea that this approach can be valid if disorder is sufficiently strong. There do of course exist also higher energy exciton states which are more delocalised, but these couple less strongly to light; these states become important only at larger densities.

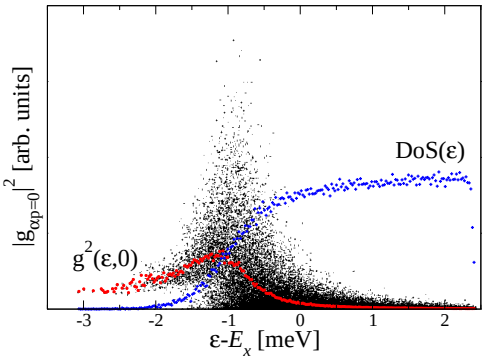

Figure 2.1: Excitonic states (black points), illustrating their energies and oscillator strengths, and the average oscillator strength (red dots) and density of states (blue dots) found by binning the data.

Connection to WIDBG model at low densities

It is worth noting that the localised exciton model can also reproduce results of the WIDBG model at very low densities. The simplest way to see this is by writing the spin 1/2 operators in terms of Holstein-Primakoff Bosons:

$$S_i^z = D_i^\dagger D_i - \frac{1}{2}, \quad S_i^+ = D_i^\dagger\sqrt{1 - D_i^\dagger D_i}, \quad S_i^- = \left(S_i^+\right)^\dagger \tag{2.12}$$

This representation is exact, but leads to a complicated nonlinear Hamiltonian. At low enough densities, the square root in Eq. (2.14) can be expanded, which then leads to an effective interaction term in a WIDBG-like model:

$$\begin{aligned} H &= \sum_i 2\epsilon_i D_i^\dagger D_i + \sum_{\mathbf{p}}\omega_{\mathbf{p}}\psi_{\mathbf{p}}^\dagger\psi_{\mathbf{p}} \\ &+ \frac{1}{\sqrt{A}}\sum_i\sum_{\mathbf{p}}\left(g_{i,\mathbf{p}}\psi_{\mathbf{p}}D_i^\dagger\left(1 - \frac{1}{2}D_i^\dagger D_i\right) + \text{H.c.}\right). \end{aligned} \tag{2.13}$$

Comparing to Eq. (2.4), this equation thus describes a saturable exciton-photon interaction, but does not have any direct exciton-exciton interactions (this is because the localised exciton model as written above neglects interactions between excitons localised on different sites.)

2.2 Mean-field theory of polariton Dicke model

After the preceding introduction, the remainder of these lectures concentrates on the properties of the localised exciton model. This model can be seen as a generalised Dicke (or more properly Tavis-Cummings) model. The Dicke model describes interactions between a single confined photon mode and a set of two-level systems. The current model is a generalisation in allowing for many photon modes, not just the $k = 0$ mode.

It is convenient in the following to make use of a fermionic representation of the spin 1/2 operators,

$$S_i^z = \frac{1}{2}\left(b_i^\dagger b_i - a_i^\dagger a_i\right), \quad S_i^+ = b_i^\dagger a_i, \quad S_i^- = \left(S_i^+\right)^\dagger. \tag{2.14}$$

This representation is exact, except that it allows for the existence of non-physical states. Physical states of the spin correspond to exactly one of the two fermionic states a, b being occupied. The zero and double occupation states are unphysical. They can however be eliminated straightforwardly by writing $\rho \to \rho \exp[i(\pi/2)(b^\dagger b + a^\dagger a)]$, which has the effect of introducing opposite signs in front of the two unphysical states, so their contribution to any expectation will vanish.

Putting aside this complication, the Hamiltonian we wish to study is of the form:

$$H - \mu N = \sum_i \left(\epsilon_i - \frac{\mu}{2}\right)(b_i^\dagger b_i - a_i^\dagger a_i) + \sum_k (\omega_k - \mu)\psi_k^\dagger \psi_k + \sum_{i,k} g_i(\psi_k^\dagger a_i^\dagger b_i + \text{H.c.}) \tag{2.15}$$

Just as for the WIDBG calculation discussed before, we can construct the mean field of this model by looking for states where we replace the photon operator $\hat{\psi}_k \to \psi_0 \delta_k$. This then leaves a quadratic problem in terms of fermionic operators. The free energy can thus be written as:

$$F = (\omega_0 - \mu)|\psi_0|^2 - k_B T \ln\left[Tr\left(e^{-\beta H_{\text{Fermi}}}\right)\right] \tag{2.16}$$

where the Fermionic part of the Hamiltonian has the form:

$$H_{\text{Fermi}} = \begin{pmatrix} b_i^\dagger & a_i^\dagger \end{pmatrix} \begin{pmatrix} \tilde{\epsilon} & g\psi \\ g\psi & -\tilde{\epsilon} \end{pmatrix} \begin{pmatrix} b_i \\ a_i \end{pmatrix}. \tag{2.17}$$

(Here we have introduced $\tilde{\epsilon} = \epsilon - \mu/2$.) The mean-field approach then demands that ψ_0 is chosen so as to minimise the free energy, and taking the derivative with respect to ψ_0^* gives the equation:

$$(\omega - \mu)\psi_0 = -g \sum_i \left\langle\!\left\langle a_i^\dagger b_i \right\rangle\!\right\rangle \tag{2.18}$$

where the angle brackets mean the thermal expectation:

$$\langle\langle \ldots \rangle\rangle = \frac{1}{\mathcal{Z}} Tr\left(\ldots e^{-\beta H}\right), \qquad \mathcal{Z} = Tr\left(e^{-\beta H}\right). \tag{2.19}$$

In order to find this expectation, we should diagonalise the Fermi problem in Eq. (2.17) by using:

$$\begin{pmatrix} b_i \\ a_i \end{pmatrix} = \begin{pmatrix} \cos(\theta) & \sin(\theta) \\ -\sin(\theta) & \cos(\theta) \end{pmatrix} \begin{pmatrix} B_i \\ A_i \end{pmatrix} \tag{2.20}$$

gives:

$$H = \begin{pmatrix} B_i^\dagger & A_i^\dagger \end{pmatrix} \begin{pmatrix} \tilde{\epsilon}\cos(2\theta) - g\psi\sin(2\theta) & \tilde{\epsilon}\sin(2\theta) + g\psi\cos(2\theta) \\ \tilde{\epsilon}\sin(2\theta) + g\psi\cos(2\theta) & -\tilde{\epsilon}\cos(2\theta) + g\psi\sin(2\theta) \end{pmatrix} \begin{pmatrix} B_i \\ A_i \end{pmatrix}. \tag{2.21}$$

This is diagonalised by choosing $\tan(2\theta) = -g\psi/\epsilon$, which then leads to $H = \sum_i E_i(B_i^\dagger B_i - A_i^\dagger A_i)$ with $E_i = \sqrt{\tilde{\epsilon}_i^2 + (g\psi)^2}$. With this Hamiltonian for the new fermionic normal modes, we may write:

$$\begin{aligned} \langle a_i^\dagger b_i \rangle &= \langle (-\sin(\theta)B_i^\dagger + \cos(\theta)A_i^\dagger)(\cos(\theta)B_i + \sin(\theta)A_i) \rangle \\ &= \frac{1}{2}\sin(2\theta)\langle A_i^\dagger A_i - B_i^\dagger B_i \rangle \\ &= -\frac{g\psi}{2E}\tanh(\beta E) \end{aligned}$$

In this last statement, we have assumed that only the two occupied states are possible states, i.e. we have neglected the unoccupied, and doubly occupied states. Were we to have included them, we would instead have got:

$$\frac{e^{\beta E} - e^{-\beta E}}{1 + e^{\beta E} + e^{-\beta E} + 1} = \frac{(e^{\beta E/2} - e^{-\beta E/2})(e^{\beta E/2} + e^{-\beta E/2})}{(e^{\beta E/2} + e^{-\beta E/2})^2} = \tanh\left(\frac{\beta E}{2}\right). \tag{2.22}$$

Restricted to the two-level systems, we find:

$$(\omega_0 - \mu)\psi = \sum_i \frac{g_i^2 \psi_0}{2E_i}\tanh(\beta E_i) \tag{2.23}$$

This is the mean-field theory of the localised exciton model of polariton condensation upon which we will build in the following lectures in order to describe the spectrum.

Chapter 3

Fluctuations in the equilibrium theory

The aim of this chapter is to discuss fluctuations about the polariton mean field theory. This includes both the population of higher energy states at non-zero temperature, as well as corrections to the ground state, as the mean-field theory is not exact. In particular, we will aim to calculate those Green's functions that correspond directly to the observable absorption and emission (i.e. photoluminescence) spectra of the condensate.

3.1 Fluctuations via Green's functions

Unlike the fluctuation spectrum for the WIDBG, in the case of the polariton Dicke model, it is not so straightforward to directly extract the spectrum by diagonalising the Hamiltonian. In particular, because of the temperature dependent occupation of the two-level systems, the mean-field state varies with temperature. As such, to find the spectrum, one requires a sum over this thermal ensemble of states, to give the possible excitation energies. The aim of this section will be to show how the Green's function approach can deliver this quantity.

Formally, to describe the observable spectrum, we are interested in something like the probability of emitting a photon at a particular energy and momentum. This may be written as:

$$P_{\text{emit}}(\omega, k) = \sum_{n,m} |\langle m|\psi_k|n\rangle|^2 \delta[\omega - (E_n - E_m)] e^{\beta(F-E_n)}, \tag{3.1}$$

i.e., this is the probability that we start in state E_n, and change to state m, by emitting a photon that carries away energy $E_n - E_m$. In the following, we will define the temperature Green's function, which can be related to this quantity. The advantage of evaluating the temperature Green's function over directly tackling the above quantity is that the definition of the temperature Green's function will allow a diagrammatic approach.

Definition and basic properties of temperature Green's function

The temperature Green's function[8] is defined by:

$$\mathcal{D}(\tau_1, \tau_2) = -\left\langle\!\left\langle T_\tau \left(\psi(\tau_1)\psi^\dagger(\tau_2)\right)\right\rangle\!\right\rangle, \tag{3.2}$$

where as before we have used

$$\langle\!\langle \ldots \rangle\!\rangle \equiv \sum_n e^{\beta(F-E_n)}\langle n|\ldots|n\rangle \equiv \frac{1}{\mathcal{Z}}\mathrm{Tr}(e^{-\beta H}\ldots) \tag{3.3}$$

(NB; in this section, we will generally assume that H means $H-\mu N$, i.e. we will work in the grand canonical ensemble, without necessarily explicitly writing $H-\mu N$.) The time ordering operator T_τ is defined by:

$$T_\tau\left(A(\tau_1)B(\tau_2)\right) = \begin{cases} +A(\tau_1)B(\tau_2) & \tau_1 > \tau_2 \\ \pm B(\tau_2)A(\tau_1) & \tau_2 > \tau_1 \end{cases}, \tag{3.4}$$

with the $\pm$ sign for bosons(fermions). Finally, we have:

$$\psi(\tau) = e^{H\tau}\psi e^{-H\tau} \tag{3.5}$$

as the Heisenberg picture operator in imaginary time.

We will restrict the above definition to $-\beta < \tau_1 - \tau_2 < \beta$, for reasons that will become clear later, and we note that the result should only depend on this difference of τ_1 and τ_2. Within this range, we may also note that if $\tau_1 < \tau_2$, then (for bosons) we may use cyclic permutations under the trace to write:

$$\begin{aligned} \mathcal{D}(\tau = \tau_1 - \tau_2) &= -\frac{1}{\mathcal{Z}}\mathrm{Tr}\left[e^{-\beta H}e^{H\tau_2}\psi^\dagger e^{-H\tau_2}e^{H\tau_1}\psi e^{-H\tau_1}\right] \\ &= -\frac{1}{\mathcal{Z}}\mathrm{Tr}\left[e^{-\beta H}e^{H(\beta+\tau_1)}\psi e^{-H(\beta+\tau_1)}e^{H\tau_2}\psi^\dagger e^{-H\tau_2}\right] \\ &= \mathcal{D}(\tau = \beta + \tau_1 - \tau_2). \end{aligned} \tag{3.6}$$

Hence, $\mathcal{D}(\tau < 0) = \mathcal{D}(\tau + \beta)$. For fermions, there is a minus sign, and so $\mathcal{G}(\tau < 0) = -\mathcal{G}(\tau + \beta)$. This means that in either case, the function can in fact be defined on $0 < \tau < \beta$, with periodic, or anti-periodic boundary conditions. Hence, the function $\mathcal{D}$ can be specified by its Fourier transform, evaluated at frequencies $\omega_n = 2\pi n T$:

$$\mathcal{D}(\omega_n) = \int_0^\beta d\tau e^{i\omega_n\tau}\mathcal{D}(\tau), \qquad \mathcal{D}(\tau) = T\sum_n e^{-i\omega_n\tau}\mathcal{D}(\omega_n). \tag{3.7}$$

For fermions, the only difference is that $\nu_n = (2n+1)\pi T$.

Relating temperature Green's function to observables

If we make use of the above properties of periodicity to write the Fourier transform, we may write:

$$\mathcal{D}(\omega_n) = -\frac{1}{\mathcal{Z}}\int_0^\beta d\tau e^{i\omega\tau}\mathrm{Tr}\left(e^{-\beta H}e^{H\tau}\psi e^{-H\tau}\psi^\dagger\right) \tag{3.8}$$

(Note that, restricted to $0 < \tau < \beta$, there is no need for the time ordering to be written). Then, writing the trace explicitly, we have:

$$\begin{aligned}\mathcal{D}(\omega_n) &= -\sum_{n,m} e^{\beta(F-E_n)}|\langle n|\psi|m\rangle|^2 \int_0^\beta e^{i\omega\tau} e^{(E_n-E_m)\tau} \\ &= -\sum_{n,m} e^{\beta(F-E_n)}|\langle n|\psi|m\rangle|^2 \frac{e^{-\beta(E_m-E_n)}-1}{i\omega-(E_m-E_n)}. \end{aligned} \tag{3.9}$$

If we now also define a similar expression:

$$\rho_L(x) = -\sum_{n,m} e^{\beta(F-E_n)}|\langle n|\psi|m\rangle|^2 \delta(x-(E_m-E_n))(1-e^{-\beta x}) \tag{3.10}$$

then we may firstly write:

$$\mathcal{D}(\omega_n) = \int_{-\infty}^{\infty} dx \frac{\rho_L(x)}{x-i\omega} \quad \Leftrightarrow \quad \Im\left[\mathcal{D}(i\omega_n = \omega + i0)\right] = \pi\rho_L(\omega), \tag{3.11}$$

and secondly, we may compare $\rho_L(x)$ to the expression for the Lumninescence spectrum given in Eq. (3.1). To make these more similar, we rewrite $\rho_L(x)$ by swapping $m \leftrightarrow n$ to give:

$$\rho_L(x) = -\sum_{n,m} e^{\beta(F-E_m)}|\langle m|\psi|n\rangle|^2 \delta(x-(E_n-E_m))(1-e^{-\beta x}), \tag{3.12}$$

and then we insert a factor of $e^{\beta(E_m-E_n)}e^{\beta x} \equiv 1$, (which is ensured by the δ function). This restores the correct Boltzmann weight, and modifies the final factor, giving:

$$\rho_L(x) = -P_{\text{emit}}(x)(e^{\beta x}-1) \quad \Leftrightarrow \quad P_{\text{emit}}(\omega) = -\rho_L(\omega)n_B(\omega). \tag{3.13}$$

Hence, $\mathcal{D}(\omega)$ can define $\rho_L(\omega)$, which is thermally populated in equilibrium, giving physical observables, such as the photoluminescence. When we come to the non-equilibrium problem, it is clear that this approach will no longer work, and in fact we will need to introduce two Green's functions to cope with the possibility of a non-thermal occupation.

Diagrammatic theory for temperature Green's functions

Having established that the temperature Green's function will provide useful information, let us now see how it may be evaluated. It is convenient to switch from the Heisenberg picture, to the interaction picture, meaning that we will write $H = H_0 + H_{\text{int}}$, where H_0 is something sufficiently simple that we may explicitly calculate the Green's function from its definition. For example, for $H_0 = \sum_k \epsilon_k \psi_k^\dagger \psi_k$, one has:

$$\mathcal{D}_0(r,\tau) = -\sum_k e^{-i\mathbf{k}\cdot\mathbf{r}-(\epsilon_k-\mu)\tau} \begin{cases} n_B(\epsilon_k-\mu) & \tau < 0 \\ 1+n_B(\epsilon_k-\mu) & \tau > 0 \end{cases} \tag{3.14}$$

which, after Fourier transforming gives $\mathcal{D}(\omega_n) = [i\omega_n - \epsilon_k + \mu]^{-1}$.

After splitting H into two parts, we introduce the interaction picture fields and the propagator $U(\tau)$:

$$\tilde{\psi}(\tau) = e^{H_0\tau}\psi e^{-H_0\tau}, \quad \psi(\tau) = U^{-1}(\tau)\tilde{\psi}(\tau)U(\tau). \tag{3.15}$$

This means $e^{-H\tau} = e^{-H_0\tau}U(\tau)$, and following standard methods, the time derivative of this equation yields:

$$\partial_\tau U = -e^{H_0\tau}H_{\rm int}e^{-H_0\tau}U, \quad U(\tau) = T_\tau \exp\left[-\int_0^\tau d\tau' \tilde{H}_{\rm int}(\tau')\right], \tag{3.16}$$

where $\tilde{H}_{\rm int}(\tau)$ is $H_{\rm int}$ in terms of the interaction picture fields. Now, if we write Eq. (3.2) in terms of the interaction picture fields and the propagators, we may drop all of the T_τ terms from the propagators, and collapse all the propagators into one, since everything occurs under a global T_τ term. Moreover, the $e^{-\beta H}$ in the definition of $\langle\langle \ldots \rangle\rangle$ may be written as $e^{-\beta H_0}U(\beta)$, and this can also be combined with the other propagators, yielding the expression:

$$\mathcal{D}(\tau_1,\tau_2) = -\frac{\left\langle\left\langle T_\tau\left(\tilde{\psi}(\tau_1)\tilde{\psi}^\dagger(\tau_2)U(\beta)\right)\right\rangle\right\rangle_0}{\langle\langle T_\tau\left(U(\beta)\right)\rangle\rangle_0}, \tag{3.17}$$

where $\langle\langle \ldots \rangle\rangle_0$ is as in Eq. (3.3), but with H replaced by H_0. This expression can now be expanded diagrammatically, by writing

$$U(\beta) \simeq 1 - \int_0^\beta d\tau' \tilde{H}_{\rm int}(\tau') + \ldots \tag{3.18}$$

and using the free Hamiltonian H_0 to evaluate the products of interaction picture fields. The restricted range of this τ integral justifies our earlier restriction of the values of τ for which we define $\mathcal{D}$. This expansion corresponds to a diagrammatic picture where $H_{\rm int}$ introduces vertices connecting particular types of fields, which are joined by lines representing the Green's functions of the free, quadratic Hamiltonian. In evaluating these diagrams it is further helpful to notice that:

$$\begin{aligned}\int_0^\beta d\tau' X(\tau_1-\tau')Y(\tau'-\tau_2) &= T^2\sum_{n,m} X_n Y_m \int_0^\beta d\tau' e^{i\omega_n(\tau_1-\tau')+i\omega_m(\tau'-\tau_2)} \\ &= T\sum_n X_n Y_n e^{i\omega_n(\tau_1-\tau_2)},\end{aligned} \tag{3.19}$$

then all internal products reduce to summations over frequencies. After this summary, we are now sufficiently prepared to tackle the polariton Dicke model.

3.2 Green's functions for the polariton Dicke model

As a reminder, we want to study the model:

$$H = \sum_i \left(\epsilon_i - \frac{\mu}{2}\right)(b_i^\dagger b_i - a_i^\dagger a_i) + \sum_k (\omega_k - \mu)\psi_k^\dagger\psi_k + \sum_{i,k} g_i(\psi_k^\dagger a_i^\dagger b_i + \text{H.c.}). \tag{3.20}$$

In the following, we will write $\tilde{\epsilon} = \epsilon - \mu/2$ and $\tilde{\omega}_k = \omega_k - \mu$ for compactness. Our aim is to consider $\hat{\psi}_k = \psi_0 \delta_k + \psi$, as we did for the simple WIDBG model above, meaning that we are looking for fluctuations in the condensed state, and we want to calculate the Green's function $\mathcal{D}_{\psi^\dagger \psi}$.

For constructing the diagrammatic perturbation theory, we will choose:

$$H_0 = \sum_i \begin{pmatrix} b_i^\dagger & a_i^\dagger \end{pmatrix} \begin{pmatrix} \tilde{\epsilon} & g\psi_0 \\ g\psi_0 & -\tilde{\epsilon} \end{pmatrix} \begin{pmatrix} b_i \\ a_i \end{pmatrix} + \sum_k (\omega_k - \mu) \psi_k^\dagger \psi_k, \quad (3.21)$$

including the effect of the condensate field on the fermionic atoms on the basis that we are capable of solving that problem by diagonalisation of the fermionic basis. As such, the interaction Hamiltonian will be

$$H_{\text{int}} = \sum_{i,k} g\psi_k b_i^\dagger a_i + \text{H.c.}, \quad (3.22)$$

and so, the diagramatic expansion of the full photon Green's function will be of the form shown in Fig. 3.1. To evaluate this series, we will note that

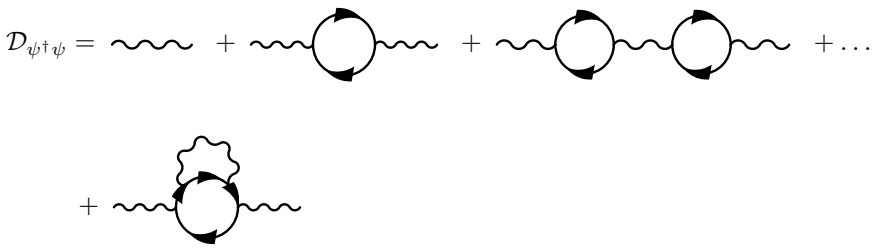

Figure 3.1: Cartoon of diagrammatic expansion of photon Green's function

the repeated diagrams in the first line of Fig. 3.1 can be summed by means of the Dyson equation; i.e. defining the self energy Σ by the set of all diagrams that cannot be disconnected by cutting a single photon line, we have:

$$\mathcal{D} = \mathcal{D}_0 + \mathcal{D}_0 \Sigma \mathcal{D} \quad \Rightarrow \quad \mathcal{D}^{-1} = \mathcal{D}_0^{-1} - \Sigma. \quad (3.23)$$

Hence, our perturbative approach will involve finding a particular approximation for Σ, based on a limited number of diagrams, and then solving the above equation for $\mathcal{D}$.

The approximation we choose is to include only the simplest diagram, a single fermion loop. This is a low density approximation scheme, since the diagrams neglected are proportional to the density of extra fluctuations. Because we consider a condensed system, the calculation of the the Green's function is slightly complicated by the need to consider both normal and

anomalous Green's functions. The normal Green's function is as defined above, and will be denoted $\mathcal{D}_{\psi^\dagger\psi}$. The anomalous Green's function is:

$$\mathcal{D}_{\psi^\dagger\psi^\dagger}(\tau_1,\tau_2) = -\left\langle\!\!\left\langle T_\tau\left(\psi^\dagger(\tau_1)\psi^\dagger(\tau_2)\right)\right\rangle\!\!\right\rangle. \tag{3.24}$$

The fact that this is non-zero arises due to the non-zero value of ψ_0, and is analogous to the existence of $\psi^\dagger\psi^\dagger$ terms in Eq. (2.18) for the WIDBG.

To deal with these Green's functions, it is easier to construct the matrix Green's function:

$$\mathcal{D} = -\left\langle\!\!\left\langle T_\tau\left[\begin{pmatrix}\psi(\tau_1)\\ \psi^\dagger(\tau_1)\end{pmatrix}\begin{pmatrix}\psi^\dagger(\tau_2) & \psi(\tau_2)\end{pmatrix}\right]\right\rangle\!\!\right\rangle = \begin{pmatrix}\mathcal{D}_{\psi^\dagger\psi} & \mathcal{D}^*_{\psi^\dagger\psi^\dagger}\\ \mathcal{D}_{\psi^\dagger\psi^\dagger} & \mathcal{D}^*_{\psi^\dagger\psi}\end{pmatrix}. \tag{3.25}$$

Given the free Hamiltonian in Eq. (3.21), only the normal components of the free Green's function exist, and so we may write:

$$\mathcal{D}_0^{-1} = \begin{pmatrix}i\omega-\tilde{\omega}_k & 0\\ 0 & -i\omega-\tilde{\omega}_k\end{pmatrix} = i\omega\sigma_3 - H \tag{3.26}$$

The two types of Green's function lead to two types of self energies in this leading approximation, which are shown in Fig. 3.2. To evaluate these we must next determine the fermionic Green's functions.

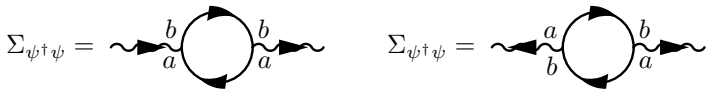

Figure 3.2: Normal and anomalous self energies, in terms of fermionic labels

For the fermionic Green's function it is also convenient to introduce a matrix notation:

$$\mathcal{G}_i = -\left\langle\!\!\left\langle T_\tau\left[\begin{pmatrix}b_i(\tau_1)\\ a_i(\tau_1)\end{pmatrix}\left(b_i^\dagger(\tau_2)a_i^\dagger(\tau_2)\right)\right]\right\rangle\!\!\right\rangle, \tag{3.27}$$

where the off-diagonal elements are only non-zero because of the coherent field ψ_0. One simple way[1] to evaluate the Green's function is to remember

[1] An alternative approach is to use the definition in Eq. (3.27) to write:

$$\begin{aligned}\partial_{\tau_1}\mathcal{G}(\tau_1,\tau_2) &= -\partial_{\tau_1}\left\langle\!\!\left\langle\theta(\tau_1-\tau_2)\begin{pmatrix}b_1b_2^\dagger & b_1a_2^\dagger\\ a_1b_2^\dagger & a_1a_2^\dagger\end{pmatrix} - \theta(\tau_2-\tau_1)\begin{pmatrix}b_2^\dagger b_1 & a_2^\dagger b_1\\ b_2^\dagger a_1 & a_2^\dagger a_1\end{pmatrix}\right\rangle\!\!\right\rangle,\\ &= -\delta(\tau_1-\tau_2)\begin{pmatrix}bb^\dagger+b^\dagger b & 0\\ 0 & aa^\dagger+a^\dagger a\end{pmatrix} + \left\langle\!\!\left\langle T_\tau\left[\begin{pmatrix}[H,b_1]\\ [H,a_1]\end{pmatrix}\left(b_2^\dagger a_2^\dagger\right)\right]\right\rangle\!\!\right\rangle,\\ &= -\delta(\tau_1-\tau_2)\mathbb{1} - H\mathcal{G},\end{aligned} \tag{3.28}$$

hence one may write $\mathcal{G}^{-1} = i\nu\mathbb{1} - H$, where H is the matrix form of the fermionic Hamiltonian. If one compares this expression to that in Eq. (3.26), one notices that here the terms $i\nu$ appear with the same sign in both elements, whereas in Eq. (3.26) the signs alternated. This is because the fermionic Hamiltonian is written in a basis of operators of the same kind (i.e. all terms to the right are creation operators), wheras the bosonic Hamiltonian involves mixing of creation and anihilation operators.

the diagonalisation used in the mean field theory:

$$\begin{pmatrix} b_i \\ a_i \end{pmatrix} = \begin{pmatrix} \cos(\theta) & \sin(\theta) \\ -\sin(\theta) & \cos(\theta) \end{pmatrix} \begin{pmatrix} B_i \\ A_i \end{pmatrix}, \tag{3.29}$$

after which the fermionic part of H_0 became:

$$H_{0,\text{fermi}} = \sum_i E_i (B_i^\dagger B_i - A_i^\dagger A_i), \tag{3.30}$$

Then, noting that $\mathcal{G}_{B^\dagger B}(\nu) = [i\nu - E_i]$, and similarly for A_i, we may write:

$$\begin{aligned} \mathcal{G}(\nu) &= \begin{pmatrix} \cos\theta & \sin\theta \\ -\sin\theta & \cos\theta \end{pmatrix} \begin{pmatrix} [i\nu - E_i]^{-1} & 0 \\ 0 & [i\nu + E_i]^{-1} \end{pmatrix} \begin{pmatrix} \cos\theta & -\sin\theta \\ \sin\theta & \cos\theta \end{pmatrix} \\ &= \frac{-1}{\nu^2 + E_i^2} \begin{pmatrix} i\nu + E\cos(2\theta) & -E\sin(2\theta) \\ -E\sin(2\theta) & i\nu - E\cos(2\theta) \end{pmatrix} \\ &= \frac{-1}{\nu^2 + E_i^2} \begin{pmatrix} i\nu + \tilde{\epsilon} & g\psi_0 \\ g\psi_0 & i\nu - \tilde{\epsilon} \end{pmatrix} \end{aligned} \tag{3.31}$$

We now have the necessary ingredients to evaluate the diagrams in Fig. 3.2. Let us demonstrate this explicitly for the normal self energy; the anomalous self energy follows identically. Summing over the frequencies of the intermediate lines, the self energy can be written as:

$$\Sigma_{\psi^\dagger\psi}(\omega) = \frac{2}{2!} T \sum_{i,\nu} \text{Tr}\left[\begin{pmatrix} 0 & 0 \\ g_i & 0 \end{pmatrix} \mathcal{G}(\nu + \omega) \begin{pmatrix} 0 & g_i \\ 0 & 0 \end{pmatrix} \mathcal{G}(\nu) \right]. \tag{3.32}$$

Here, the matrices represent the parts of the perturbation Hamiltonian proportional to ψ and to $\psi^\dagger$. Inserting the form of $\mathcal{G}$, and evaluating the matrix products this becomes:

$$\begin{aligned} \Sigma_{\psi^\dagger\psi}(\omega) &= T \sum_{i,\nu} \frac{g_i^2}{\left[(\nu+\omega)^2 + E_i^2\right]\left[\nu^2 + E_i^2\right]} \\ &\qquad \times \text{Tr}\left[\begin{pmatrix} 0 & 0 \\ i(\nu+\omega) + \tilde{\epsilon}_i & g\psi_0 \end{pmatrix} \begin{pmatrix} g\psi_0 & i\nu - \tilde{\epsilon}_i \\ 0 & 0 \end{pmatrix} \right] \\ &= T \sum_{i,\nu} \frac{g_i^2 \left[i\nu - \tilde{\epsilon}_i\right]\left[i(\omega+\nu) + \tilde{\epsilon}_i\right]}{\left[(\nu+\omega)^2 + E_i^2\right]\left[\nu^2 + E_i^2\right]}. \end{aligned} \tag{3.33}$$

Using standard contour integration methods[2] to evaluate this sum we the final expression for $\Sigma_{\psi^\dagger\psi}$ and similarly for the anomalous term. Assuming all two-level systems have identical values of ϵ and g, we find:

$$\Sigma_{\psi^\dagger\psi}(\omega) = ng^2 \frac{\tanh(\beta E)}{E} \left(\frac{-i\tilde{\epsilon}\omega - E^2 - \tilde{\epsilon}^2}{\omega^2 + 4E^2} \right), \tag{3.35}$$

$$\Sigma_{\psi^\dagger\psi^\dagger}(\omega) = ng^2 \frac{\tanh(\beta E)}{E} \left(\frac{g^2\psi_0^2}{\omega^2 + 4E^2} \right), \tag{3.36}$$

[2]Making use of the formula:

$$T \sum_n f(\nu_n = (2n+1)\pi T) = \int_C \frac{dz}{2\pi i} f(\nu = -iz) 2\tanh\left(\frac{\beta z}{2}\right) \tag{3.34}$$

where n is the number of two-level systems. Hence, the fluctuation Green's function is to be found by inverting

$$\mathcal{D}^{-1} = \begin{pmatrix} i\omega - \tilde{\omega}_k - \Sigma_{\psi^\dagger\psi}(\omega) & -\Sigma^*_{\psi^\dagger\psi^\dagger}(\omega) \\ -\Sigma_{\psi^\dagger\psi^\dagger}(\omega) & -i\omega - \tilde{\omega}_k - \Sigma^*_{\psi^\dagger\psi}(\omega) \end{pmatrix} \tag{3.37}$$

Properties of the fluctuation spectrum

For the above results, it is in fact straightforward to calculate a spectrum, since the expressions for Σ are rational functions of ω. This means that when we calculate $\mathcal{D}$, it will also be a rational function of ω, and so after analytic continuation as described in Eq. (3.11), there will be a series of δ function peaks, at the poles of $\det(\mathcal{D}^{-1})$. The location of these poles are shown in Fig. 3.3.

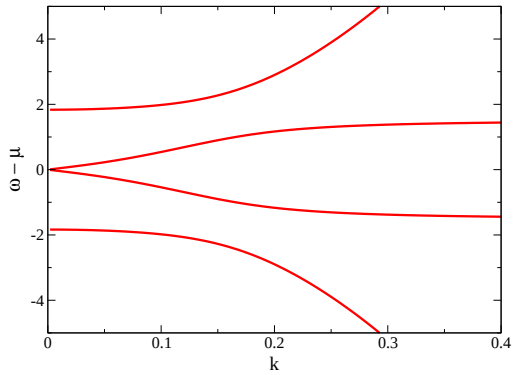

Figure 3.3: Spectrum of normal modes in the condensed system

For the WIDBG, the equivalent poles would have been at $\omega - \mu = \pm\sqrt{\epsilon_k(\epsilon_k + 2\mu)}$. The fact that the condensed system has symmetric modes above and below the chemical potential reflects the mixing of particle- and hole-like excitations by the anomalous self energy. (Note that although the modes are symmetric, the weights with which each contribute to the Green's function are not, and for large k, only the positive frequency modes contribute.)

As a condensate breaks the global phase symmetry of the original Hamiltonian, there is a gapless mode associated with this spontaneously broken symmetry. In the case of a condensate, this statement can be made slightly more specific: the fact that $\langle\psi_k\rangle = 0$ for the fluctuation modes, can be shown show (see e.g. [16]) to be equivalent to the Hugenholtz-Pines relation that $\mathcal{D}^{-1}_{\psi^\dagger\psi}(0,0) = \mathcal{D}^{-1}_{\psi^\dagger\psi^\dagger}(0,0)$ or equivalently that:

$$\mu = \omega_0 + \Sigma_{\psi^\dagger\psi}(\omega = 0, k = 0) - \Sigma_{\psi^\dagger\psi^\dagger}(\omega = 0, k = 0). \tag{3.38}$$

This means that at $\omega = 0, k = 0$, the Green's function in Eq. (3.37) disappears.[3]. It is instructive to see how Eq. (3.38) is satisfied in the current

[3]The standard form of the Hugenholtz-Pines relation assumes that ω_k starts from zero; the form in Eq. (3.38) generalised this to non-zero $\omega_{k=0}$.

case. From Eq. (3.35) we may write:

$$\begin{aligned}&\tilde{\omega}_0 + \Sigma_{\psi^\dagger\psi}(\omega = 0, k = 0) - \Sigma_{\psi^\dagger\psi^\dagger}(\omega = 0, k = 0) \\ &= \tilde{\omega}_0 + ng^2 \frac{\tanh(\beta E)}{E}\left(\frac{-E^2 - \tilde{\epsilon}^2 - g^2\psi_0^2}{4E^2}\right) = \tilde{\omega}_0 - ng^2\frac{\tanh(\beta E)}{2E}. \quad (3.39)\end{aligned}$$

The condition for this final expression to vanish is the mean-field condition that was previously discussed, hence the condition for condensation implies the spectrum will be gapless.

Compared to the WIDBG, the spectrum in Fig. 3.3 has two additional gapped modes, that arise due to the original Hamiltonian involving two coupled dynamical degrees of freedom. If we allow the energies and the coupling strengths of individual two-level systems to vary, then each term in the sum in Eq. (3.35) will add a different pole; in the limit of many terms i, this means that the discrete poles will be replaced by branch cuts; this can be seen by plotting the spectral density, $-\rho_L(\omega)$, as in Fig. 3.4.

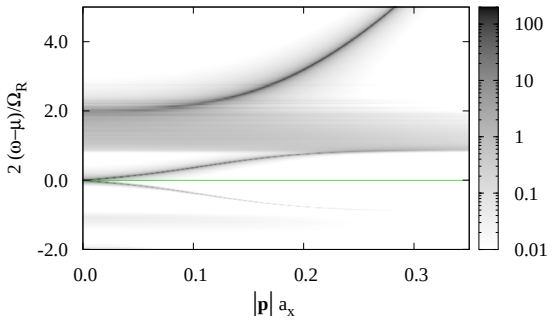

Figure 3.4: Spectral weight, $-\rho_L(\omega)$ in the case of varying energies and couplings strengths between the two-level systems and light.

Chapter 4

Non-equilibrium model and diagram technique.

Having discussed the equilibrium mean field theory and fluctuations, our aim now is to show how to derive a similar treatment of the non-equilibrium system. Therefore, we will first introduce a model of the system driven out of equilibrium by the pumping and decay, and then consider what a non-equilibrium mean-field theory should mean. Then, in order to evaluate correlation functions required for this mean field condition, we will introduce the non-equilibrium diagram technique, which will also allow us to consider fluctuations in the following chapters.

4.1 The model

In order to drive the system out of equilibrium, we consider the model $H = H_{\rm sys} + H_{\rm sys,bath} + H_{\rm bath}$, where $H_{\rm sys}$ is the polariton Dicke model as before:

$$H_{\rm sys} = \sum_i \epsilon_i (b_i^\dagger b_i - a_i^\dagger a_i) + \sum_k \omega_k \psi_k^\dagger \psi_k + \sum_{i,k} g_i (\psi_k^\dagger a_i^\dagger b_i + \text{H.c.}), \qquad (4.1)$$

and $H_{\rm sys,bath}$ describes coupling of these fields to bath degrees of freedom:

$$H_{\rm sys,bath} = \sum_{n,i} \Gamma_{n,i} \left(a_i^\dagger A_n + b_i^\dagger B_n + \text{H.c.} \right) + \sum_{p,k} \zeta_{p,k} \left(\psi_k^\dagger \Psi_p + \text{H.c.} \right). \quad (4.2)$$

The bath modes are taken to have the Hamiltonian of free particles. Schematically the idea is illustrated in Fig. 4.1.

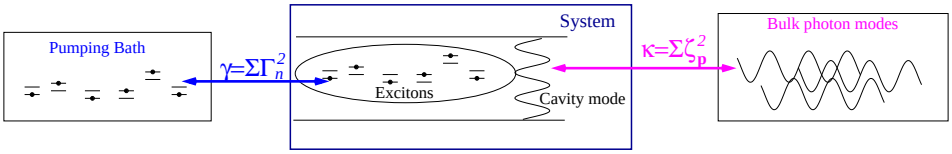

Figure 4.1: Cartoon of system coupled to pumping and decay baths.

These baths, described by the fermionic operators A_n, B_n and bosonic operators Ψ_p can transfer particles and energy into and out of the system. We will assume that they are baths in the sense that the couplings ζ, Γ are weak, but there are many bath modes for each system mode, so that the net influence of the bath on the system is significant, while the influence of the system on a given bath mode is weak (but non-zero). Explicitly, this will mean we calculate the linear response of the bath to the system, evaluating the bath Green's functions assuming free baths. In fact, this assumption is not required for our model of pumping, as the linear coupling between the system and the reservoir means that the only possible contributions are the linear response. i.e., while the small system-reservoir coupling means that no corrections to linear response are important, the structure of the coupling means that no such corrections exist.

Note that in the following, because we have explicitly coupled the system to baths, we will work with the true Hamiltonian, rather than $H - \mu N$.

4.2 Outline of mean-field theory

In producing the mean field theory, we may no longer think about minimising free energy, since the entropy cost of a given amount of system energy is no longer fixed once we introduce multiple baths. Hence, whereas in equilibrium the occupation of a state depended only on its energy, here, the occupation depends on a balance of the rates of energy transfer to and from the bath. Instead of minimising energy, we will look for self consistent steady states, and will later determine which of these are stable. As before, we will consider the steady state $\langle \psi_k \rangle = \psi_0 \delta_k \exp(-i\mu t) = \delta_k \psi_0(t)$. Here, μ is introduced as part of the mean-field ansatz, indicating the frequency of the condensate. In equilibrium this frequency would be the chemical potential, hence the choice of notation.

Our ansatz must satisfy the semiclassical approximation to the Heisenberg equation: $\langle i\partial_t \psi \rangle = \langle [\psi, H] \rangle$, and so:

$$\mu\psi_0(t) = \omega_0\psi_0(t) + \sum_i g_i \langle a_i^\dagger(t) b_i(t) \rangle + \sum_p \zeta_{p,0} \langle \Psi_p(t) \rangle. \tag{4.3}$$

Most of our effort will be dedicated to finding $\langle a_i^\dagger b_i \rangle$ for the non-equilibrium system, but as a warmup, let us show how to derive $\langle \Psi_p \rangle$ making use of bath Green's functions. One should note that while more direct ways to find this expectation exist, the following approach is intended to introduce the notation and approach relevant to the calculation of the fermionic correlations, and the Green's functions describing the fluctuations.

Decay bath and $\langle \Psi_p \rangle$

Note that although the effect of the system on the bath is weak, it is not vanishing, and so $\langle \Psi_p \rangle$ exists because of the linear response of the bath. Just as for the temperature Green's functions, it is useful to work in the

interaction picture (but now, in real time), hence we write:

$$\Psi_p(t) = U^{-1}(t)\tilde{\Psi}_p(t)U(t), \qquad e^{-iHt} = e^{-iH_0t}U(t), \tag{4.4}$$

and so we have:

$$U(t) = T\exp\left(-i\int_{-\infty}^{t} dt' \tilde{H}_{\rm int}(t')\right). \tag{4.5}$$

In the present problem, $H_{\rm int} = \sum_p \zeta_{p,0}\psi_0(t)\Psi_p^\dagger + \text{H.c.}$, and so the linear response to the bath gives:

$$\langle\Psi_p(t)\rangle = \langle\tilde{\Psi}_p(t)\rangle - i\zeta_{p,0}\int^t dt'\psi_0(t')\left\langle\left[\tilde{\Psi}_p(t), \tilde{\Psi}_p^\dagger(t')\right]\right\rangle + \mathcal{O}(\zeta^2). \tag{4.6}$$

In this expression, the commutator arises because we have factors of U and U^{-1} either side of $\tilde{\Psi}_p$. We have neglected anomalous correlators (as we assume free bath Green's functions), and our assumption of weak bath coupling means that ultimately we preserve terms like $\sum_p \zeta_{p,0}^2$, but neglect any higher powers of ζ.

The above equation can naturally be written in terms of the retarded Green's function, which will be one of the two crucial ingredients of the non-equilibrium diagram technique:

$$D^R_{\Psi_p^\dagger\Psi_p}(t,t') = -i\theta(t-t')\left\langle\left[\tilde{\Psi}_p(t), \tilde{\Psi}_p^\dagger(t')\right]\right\rangle, \tag{4.7}$$

giving:

$$\sum_p \zeta_{p,0}\langle\Psi_p(t)\rangle = \sum_p \zeta_{p,0}^2\int dt' D^R_{\Psi_p^\dagger\Psi_p}(t,t')\psi_0(t'). \tag{4.8}$$

For a free bath, one may write $\tilde{\Psi}_p(t) = e^{-i\omega_p^\zeta t}\Psi_p$, and so:

$$D^R_{\Psi_p^\dagger\Psi_p}(t,t') = -i\theta(t-t')e^{-i\omega_p^\zeta(t-t')}. \tag{4.9}$$

If we now make a Markovian approximation for the bath density of states, we may write:

$$\sum_p \zeta_{p,0}^2 e^{-i\omega_p^\zeta(t-t')} = 2\kappa\delta(t-t') \tag{4.10}$$

giving a simple expression for the effect of the decay bath. Putting this all together the mean field condition is:

$$(\omega_0 - \mu - i\kappa)\psi_0 e^{-i\mu t} = -\sum_i g_i\langle a_i^\dagger(t)b_i(t)\rangle \tag{4.11}$$

4.3 Non-equilibrium Green's functions

In general, the non-equilibrium diagram approach requires two types of Green's function, to determine separately the spectrum of excitations, and the occupation of this spectrum. We will choose these two Green's functions

to be the retarded Green's function (as above), and the Keldysh Green's function:

$$D^K = -i \left\langle \left[\psi(t), \psi^\dagger(t') \right]_+ \right\rangle . \tag{4.12}$$

These Green's functions define respectively the spectrum of possible modes, and in addition, the occupation of this spectrum. For fermions, the commutator and anticommutator are interchanged. Note that any linearly independent combination of these would be sufficient; our choice is however motivated by the ability to produce a diagrammatic expansion for these Green's functions. In some cases we will also refer to the advanced Green's function, which is the Hermitian conjugate (including transposition of times) of the retarded Green's function.[1]

The method to produce a diagrammatic expansion of the Green's function is based on introducing the Keldysh closed-time path contour, shown in Fig. 4.2. Each point on this contour is labelled by $(t, \{f, b\})$, where the f, b

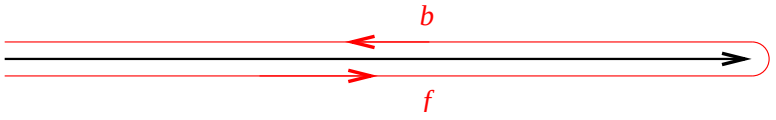

Figure 4.2: Keldysh time path contour.

labels whether it is on the forward or backward branch. We then introduce the contour time ordering T_c, such that fields on the backward contour are always later than those on the forward contour, and that pairs of fields on the backward contour should appear in reverse order. By adding these labels and this time ordering, one can select particular desired time-orderings,

[1] As an aside, it is worth noting that in equilibrium all of these Green's functions can be given in terms of the $\rho_L(x)$ in Eq. (3.10). For the retarded Green's function we may write:

$$\begin{aligned} D^R(\omega) &= -i \int_0^\infty dt e^{i\omega t} \left\langle \psi(t)\psi^\dagger(0) - \psi^\dagger(0)\psi(t) \right\rangle \\ &= -i \sum_{n,m} e^{\beta F} |\langle n|\psi|m\rangle|^2 \left(e^{-\beta E_n} - e^{-\beta E_m} \right) \int_0^\infty dt e^{i\omega t} e^{i(E_n - E_m)t} \\ &= \sum_{n,m} e^{\beta(F-E_n)} |\langle n|\psi|m\rangle|^2 \left(1 - e^{-\beta(E_m - E_n)} \right) \frac{1}{(\omega - E_m + E_n) + i0} \qquad (4.13) \\ &= \int dx \frac{\rho_L(x)}{x - \omega - i0} \qquad (4.14) \end{aligned}$$

and similarly,

$$\begin{aligned} D^K(\omega) &= -i \sum_{n,m} e^{\beta(F-E_n)} |\langle n|\psi|m\rangle|^2 \left(1 + e^{-\beta(E_m - E_n)} \right) 2\pi\delta(\omega - E_m + E_n) \\ &= (2\pi i) \left(\frac{1 + e^{-\beta\omega}}{1 - e^{-\beta\omega}} \right) \rho_L(\omega) \\ &= (2\pi i)(2n_B(\omega) + 1)\rho_L(\omega) = \left[D^R(\omega) - D^A(\omega) \right] (2n_B(\omega) + 1). \qquad (4.15) \end{aligned}$$

Hence, in equilibrium, knowledge of $\rho_L(x)$ and the thermal distribution function would determine these Green's functions.

e.g.

$$D^{>}(t) = -i\left\langle T_c\left(\psi(t,b)\psi^\dagger(0,f)\right)\right\rangle = -i\langle\psi(t,r)\psi^\dagger(0,0)\rangle. \tag{4.16}$$

Our aim is however to calculate the retarded and Keldysh Green's functions, for which it is helpful to introduce

$$\psi_\pm = \frac{\psi(t,f)\pm\psi(t,b)}{\sqrt{2}}, \tag{4.17}$$

in terms of which we can construct a matrix of the required Green's functions:

$$D = -i\left\langle T_c\begin{pmatrix}\psi_+(t)\\ \psi_-(t)\end{pmatrix}\begin{pmatrix}\psi_+^\dagger(t) & \psi_-^\dagger(t)\end{pmatrix}\right\rangle = \begin{pmatrix}D^K & D^R\\ D^A & 0\end{pmatrix}. \tag{4.18}$$

As an illustration, let us demonstrate that this definition correctly recovers the retarded Green's function. Writing out the $\pm$ fields explicitly, and taking account of time orderings one finds:

$$\begin{aligned} D^R &= -i\left\langle T_c\left(\frac{\psi(t,f)+\psi(t,b)}{\sqrt{2}}\right)\left(\frac{\psi^\dagger(0,f)-\psi^\dagger(0,b)}{\sqrt{2}}\right)\right\rangle \\ &= -\frac{i}{2}\left\langle \psi(t)\psi^\dagger(0)-\psi^\dagger(0)\psi(t)+\begin{cases}\psi(t)\psi^\dagger(0)-\psi^\dagger(0)\psi(t) & t>0\\ \psi^\dagger(0)\psi(t)-\psi(t)\psi^\dagger(0) & t<0\end{cases}\right\rangle \end{aligned} \tag{4.19}$$

Thus, for $t>0$ the terms in the expectation add, cancelling the factor of $1/2$ in front, whereas for $t<0$ the terms cancel.

Since this an expectation of a time ordered product of fields, we may construct a diagrammatic expansion as we did in equilibrium. As there, it will be useful to use the Dyson equation to re-sum the perturbation series, which requires knowing the form of the inverse Green's function. By writing:

$$\begin{pmatrix}0 & \left[D^A\right]^{-1}\\ \left[D^R\right]^{-1} & \left[D^{-1}\right]^K\end{pmatrix}\begin{pmatrix}D^K & D^R\\ D^A & 0\end{pmatrix} = \begin{pmatrix}1 & 0\\ 0 & 1\end{pmatrix}, \tag{4.20}$$

one finds this is satisfied by $\left[D^{-1}\right]^K = -\left[D^R\right]^{-1}D^K\left[D^A\right]^{-1}$. Hence, for a free bosonic field, thermally populated we find that:

$$\left[D^R\right]^{-1} = \omega-\omega_k+i0, \quad \left[D^{-1}\right]^K = (2i0)(2n_B(\omega)+1). \tag{4.21}$$

The infinitesimal quantity in the inverse Keldysh component can cause difficulties, but for an open system it does not, since it is dwarfed by effects of coupling to baths.

In order to construct the diagrammatic perturbation expansion, we need only one further piece of formalism. That is to note that to relate interaction and Heisenberg picture fields on the closed real time contour, one

requires:

$$D = -i\left\langle T_c\left[\begin{pmatrix}\tilde{\psi}_+(t)\\ \tilde{\psi}_-(t)\end{pmatrix}\begin{pmatrix}\tilde{\psi}_+^\dagger(t) & \tilde{\psi}_-^\dagger(t)\end{pmatrix}U\right]\right\rangle, \tag{4.22}$$

$$U = \exp\left(-i\int_C dt\tilde{H}_{\rm int}(t)\right), \tag{4.23}$$

where we must evaluate:

$$\int_C dt\tilde{H}_{\rm int} = \int_{-\infty}^{\infty} dt\left[\tilde{H}_{int,f}(t) - \tilde{H}_{int,b}(t)\right]. \tag{4.24}$$

4.4 Application to polariton Dicke model

We now apply the above methods to the polariton problem. We want to evaluate $\langle a_i^\dagger(t)b_i(t)\rangle$, which can be seen to be equal to:

$$\frac{1}{2}\left\langle\left[b_i(t), a_i^\dagger(t)\right]\right\rangle = \frac{i}{2}G^K_{a_i^\dagger b_i}(t,t) = \frac{i}{2}\int\frac{d\nu}{2\pi}G^K_{a_i^\dagger b_i}(\nu), \tag{4.25}$$

noting that for fermions, commutators and anti-commutators are swapped in the definitions of Green's functions. Our task is thus to find the matrix of fermionic Green's functions in the 4×4 space associated with the combination of the a, b space, and the $\pm$ space associated with Keldysh vs retarded Green's functions.

For the free fermion Green's functions, we will worry only about the inverse retarded Green's function, since the inverse Keldysh part is infinitesimal, and will be dwarfed by the effect of the bath. We can use the same method as in Eq. (3.31), of diagonalising the fermionic part of H_0, and the free retarded Greens function of mode with energy E, $[\nu - E + i0]^{-1}$. Before doing this, we must first note that with the time-dependent ansatz, $\psi_0(t) = \psi_0 e^{-i\mu t}$, the diagonalisation of the Hamiltonian becomes more complicated. However, this time dependence can be eliminated by a gauge transformation:

$$H \to H - \frac{\mu}{2}\left[\sum_i\left(b_i^\dagger b_i - a_i^\dagger a_i\right) + \sum_n\left(B_n^\dagger B_n - A_n^\dagger A_n\right)\right]. \tag{4.26}$$

This has the effect of changing $b \to be^{-i\mu t/2}, a \to ae^{i\mu t/2}$, which removes the time dependence of the mean-field photon to fermion coupling. The gauge transformation for the bath modes ensure no time dependence is introduced in the coupling between the fermions and their bath. The net result is that the free Hamiltonian involves $\epsilon_i \to \tilde{\epsilon}_i = \epsilon_i - \mu/2$, and the bath correlation functions are also shifted in frequency by $\mu/2$.

$$G_0^R(\nu) = \frac{1}{(\nu+i0)^2 - E_i^2}\begin{pmatrix}\nu+\tilde{\epsilon}+i0 & g\psi_0\\ g\psi_0 & \nu-\tilde{\epsilon}+i0\end{pmatrix} \tag{4.27}$$

$$\left[G_0^R\right]^{-1} = \begin{pmatrix}\nu-\tilde{\epsilon}+i0 & -g\psi_0\\ -g\psi_0 & \nu+\tilde{\epsilon}+i0\end{pmatrix}. \tag{4.28}$$

We must then determine the self energy due to coupling to the baths. The appropriate part of interaction Hamiltonian is the fermionic part of $H_{\text{sys,bath}}$, which gives:

$$\begin{aligned}\int_C dt\tilde{H}_{\text{int}} &= \int_{-\infty}^{\infty} dt \left[\tilde{a}_i^\dagger(t,f)\tilde{A}_n(t,f) - \tilde{a}_i^\dagger(t,b)\tilde{A}_n(t,b) + \ldots\right] \\ &= \int_{-\infty}^{\infty} dt \left[\tilde{a}_{i+}^\dagger(t)\tilde{A}_{n-}(t) + \tilde{a}_{i-}^\dagger(t)\tilde{A}_{n+}(t) + \ldots\right]. \end{aligned} \tag{4.29}$$

As the baths each couple to a single fermionic mode, let us concentrate of $\Sigma_{a^\dagger a}$, which in matrix form is:

$$\Sigma_{a^\dagger a} = \begin{pmatrix} \Sigma_{a^\dagger a}^{++} & \Sigma_{a^\dagger a}^{+-} \\ \Sigma_{a^\dagger a}^{-+} & \Sigma_{a^\dagger a}^{--} \end{pmatrix}. \tag{4.30}$$

An example diagram is: $\Sigma_{a^\dagger a}^{-+} =$ 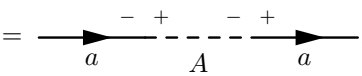

, giving the equations:

$$\begin{aligned}
\Sigma_{a^\dagger a}^{++}(t,t') &= \sum_n \Gamma_{i,n}^2 G_{A^\dagger A}^{--} = 0 \\
\Sigma_{a^\dagger a}^{-+}(t,t') &= \sum_n \Gamma_{i,n}^2 G_{A^\dagger A}^{+-} = -i\sum_n \Gamma_{i,n}^2 \theta(t-t') e^{-i\nu_n^\Gamma (t-t')} = -i\gamma\delta(t-t') \\
\Sigma_{a^\dagger a}^{+-}(t,t') &= \sum_n \Gamma_{i,n}^2 G_{A^\dagger A}^{-+} = +i\sum_n \Gamma_{i,n}^2 \theta(t'-t) e^{+i\nu_n^\Gamma (t-t')} = +i\gamma\delta(t-t') \\
\Sigma_{a^\dagger a}^{--}(t,t') &= \sum_n \Gamma_{i,n}^2 G_{A^\dagger A}^{++} = -i\sum_n \Gamma_{i,n}^2 [1-2n_A(\nu_n^\Gamma)] e^{-i\nu_n^\Gamma (t-t')} = -2i\gamma \breve{F}_A(t-t'),
\end{aligned}$$

where in the last expression we have used:

$$\breve{F}_A(t) = \int \frac{d\nu}{2\pi} e^{-i\nu t} F_A(\nu), \qquad F_A(\nu) = 1 - 2n_A(\nu), \tag{4.31}$$

where the form of the occupation function F comes from the form of the equal-time Keldysh Green's function $F_A(\nu_n^\Gamma) = \langle A_n A_n^\dagger - A_n^\dagger A_n \rangle$. In frequency space, we therefore have:

$$\Sigma_{a^\dagger a}(\nu) = \begin{pmatrix} 0 & i\gamma \\ -i\gamma & -2i\gamma F_A(\nu) \end{pmatrix}. \tag{4.32}$$

Combining this with the free Green's functions, we may write the entire inverse Green's function in the basis (b_+, a_+, b_-, a_-) as:

$$G^{-1}(\nu) = \begin{pmatrix} 0 & 0 & \nu - \tilde{\epsilon} - i\gamma & -g\psi_0 \\ 0 & 0 & -g\psi_0 & \nu + \tilde{\epsilon} - i\gamma \\ \nu - \tilde{\epsilon} + i\gamma & -g\psi_0 & 2i\gamma F_B(\nu) & 0 \\ -g\psi_0 & \nu + \tilde{\epsilon} + i\gamma & 0 & 2i\gamma F_A(\nu) \end{pmatrix}. \tag{4.33}$$

Clearly, if ψ_0 is zero then this is two uncoupled fermionic problems. However for non-zero ψ_0, the Keldysh Green's functions and hence the occupations of the two fermions get mixed.

To complete our analysis, we may use the block structure of the above matrix to write:

$$\mathcal{G}^K(\nu) = -\frac{2i\gamma}{[(\nu+i\gamma)^2 - E^2][(\nu-i\gamma)^2 - E^2]} \times \begin{pmatrix} \nu+\tilde{\epsilon}+i\gamma & g\psi_0 \\ g\psi_0 & \nu-\tilde{\epsilon}+i\gamma \end{pmatrix} \begin{pmatrix} F_B(\nu) & 0 \\ 0 & F_A(\nu) \end{pmatrix} \begin{pmatrix} \nu+\tilde{\epsilon}-i\gamma & g\psi_0 \\ g\psi_0 & \nu-\tilde{\epsilon}-i\gamma \end{pmatrix}, \tag{4.34}$$

and so, picking out the $G^K_{a^\dagger b}$ component, we get:

$$(\omega_0 - \mu - i\kappa)\psi_0 = \sum_i g_i^2 \psi_0 \gamma \int \frac{d\nu}{2\pi} \frac{(F_B+F_A)\nu + (F_B-F_A)(\tilde{\epsilon}+i\gamma)}{[(\nu-E)^2+\gamma^2][(\nu+E)^2+\gamma^2]}. \tag{4.35}$$

The significance of this form will be discussed in the next section, by considering how it contains as limits both the equilibrium results and the behaviour of a standard laser.

Chapter 5

Properties of the non-equilibrium mean field theory

At the end of the previous section, we had derived the mean-field condition for the non-equilibrium system:

$$(\omega_0 - \mu - i\kappa)\psi_0 = \sum_i g_i^2 \psi_0 \gamma \int \frac{d\nu}{2\pi} \frac{(F_B + F_A)\nu + (F_B - F_A)(\tilde{\epsilon} + i\gamma)}{[(\nu - E)^2 + \gamma^2][(\nu + E)^2 + \gamma^2]}. \quad (5.1)$$

Our aim now is first to understand the meaning of this expression, and then to consider fluctuations about this expression. One thing to note is that, since this considered equilibrium of the fermions, coupled only to the condensed bosons and the pumping bath, nothing as yet involved the occupation of the bosonic bath. When considering fluctuations about the mean-field theory however, this distribution function will enter. It is worth noting that since it is physically appropriate to consider an empty decay bath, the fact that the population of the bath does not enter the mean-field condition will not cause any difficulties; in a case where the occupation of the bath was important, one would need to rethink the mean-field approach to take account of decay bath induced population.

To understand the mean-field theory written so far, we consider first two extreme limits, to show that Eq. (5.1) contains both the equilibrium results and also contains the results of a simple laser theory — a theory we will come back to again when discussing the effect of fluctuations.

Pumping bath distributions

Before considering the limits, we must briefly discuss the functions $F_{A,B}(\nu) = 1 - 2n_{A,B}(\nu)$. We will choose these to be in thermal equilibrium, but choose different chemical potentials for the two baths. This corresponds to allowing the bath to try to set a particular level of inversion of the two-level systems. This is a somewhat crude model of the pumping, but leads to the particularly tractable approach that we have discussed. In addition, noting that the fermionic states were supposed to represent two-level systems, we

take the occupations to satisfy $n_A + n_B = 1$. This therefore requires that we have:

$$F_{A,B}(\nu) = \tanh\left[\frac{\beta}{2}\left(\nu \pm \frac{\mu_B}{2}\right)\right], \tag{5.2}$$

where μ_B is an adjustable pumping bath chemical potential. This is before we make the gauge transformation required to eliminate the time dependence of the photon field; after this transformation, we have that $\mu_B \to \mu_B - \mu$. Schematically, this situation is illustrated in Fig. 5.2; one can see that $F_A(-\epsilon) + F_B(\epsilon) = 2[1 - n_A(-\epsilon) - n_B(\epsilon)] = 0$.

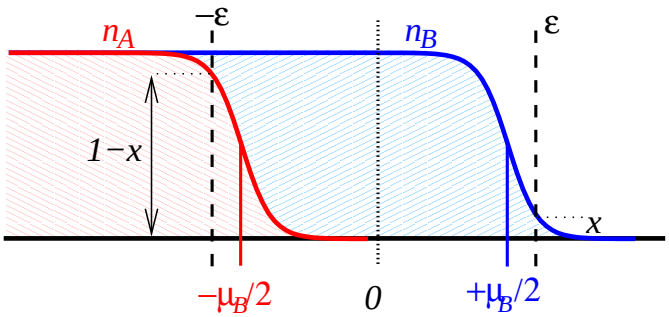

Figure 5.1: Occupation functions for the pumping baths, chosen to set total occupation of two modes to one, while varying the degree of inversion.

5.1 Comparison to equilibrium result

In order to recover the equilibrium limit, we must consider $\gamma, \kappa \to 0$. Because we have only included the coupling between mean-field photons and the decay bath in our mean-field theory, there is no way that a thermal distribution can be set by the decay bath. On the other hand, the pumping bath can do so, hence to recover an equilibrium distribution at non-zero temperature we should take $\kappa \to 0$ first, and then $\gamma \to 0$. If we take $\kappa \to 0$, then the imaginary part of the right hand side of Eq. (5.1) must vanish, so:

$$0 = \gamma \sum_i g_i^2 \psi_0 \gamma \int \frac{d\nu}{2\pi} \frac{(F_B - F_A)}{[(\nu - E)^2 + \gamma^2][(\nu + E)^2 + \gamma^2]}. \tag{5.3}$$

In order to solve this, while not restricting the range of solutions of the real part, one must choose $F_B = F_A$. In terms of the distribution functions written in Eq. (5.2), this clearly means $\mu = \mu_B$. Physically, this means that in the absence of decay, the chemical potential of the condensate matches the pumping bath.

After fixing μ, the remaining part of the equation becomes:

$$(\omega_0 - \mu_B)\psi_0 = \sum_i g_i^2 \psi_0 \gamma \int \frac{d\nu}{2\pi} \frac{2\tanh(\beta\nu/2)\,\nu}{[(\nu - E)^2 + \gamma^2][(\nu + E)^2 + \gamma^2]}. \tag{5.4}$$

We may then take the limit of small γ, by writing:

$$\frac{2\gamma\nu}{[(\nu-E)^2+\gamma^2][(\nu+E)^2+\gamma^2]} = \frac{1}{4E}\left[\frac{2\gamma}{(\nu-E)^2+\gamma^2} - \frac{2\gamma}{(\nu+E)^2+\gamma^2}\right] \tag{5.5}$$

$$\Rightarrow \frac{2\pi}{4E}\left[\delta(\nu-E)-\delta(\nu+E)\right], \tag{5.6}$$

hence we find:

$$\begin{aligned}(\omega_0-\mu_B)\psi_0 &= \sum_i \frac{g_i^2\psi_0}{4E}\int d\nu \tanh\left(\frac{\beta\nu}{2}\right)\left[\delta(\nu-E)-\delta(\nu+E)\right] \\ &= \sum_i \frac{g_i^2\psi_0}{2E}\tanh\left(\frac{\beta E}{2}\right).\end{aligned} \tag{5.7}$$

This is the equilibrium result, but with the two-level constraint on the fermions imposed only on average.[1]

5.2 High temperature limit and laser theory

The second limit we will consider can be labelled either as the high temperature limit or as the Markovian limit. This limit means taking F_A and F_B to be numbers, i.e. independent of frequency. The sense in which this is a Markovian approximation is that if we go back to the Keldysh self energies,

$$\Sigma^{--}_{a^\dagger a}(t,t') = \sum_n \Gamma^2_{i,n} G^{++}_{A^\dagger A} = -i\sum_n \Gamma^2_{i,n}[1-2n_F(\nu_n^\Gamma)]e^{-i\nu_n^\Gamma(t-t')}, \tag{5.9}$$

then a fully Markovian approximation would be to write this as:

$$\Sigma^{--}_{a^\dagger a}(t,t') = -2i\gamma F_A\delta(t-t'). \tag{5.10}$$

As such, we should note that our general approach is Markovian only for the density of states of the bath, but non-Markovian for the noise distribution.[2]

[1] Allowing for zero and doubly occupied fermionic states, the inversion $\langle b^\dagger b - a^\dagger a\rangle$ can be written as:

$$\frac{e^{\beta E}-e^{-\beta E}}{1+e^{\beta E}+e^{-\beta E}+1} = \frac{(e^{\beta E/2}-e^{-\beta E/2})(e^{\beta E/2}+e^{-\beta E/2})}{(e^{\beta E/2}+e^{-\beta E/2})^2} = \tanh\left(\frac{\beta E}{2}\right). \tag{5.8}$$

[2] In terms of quantum statistical approaches, this means that we assume that the Quantum noise from the bath, F, obeys

$$\left\langle\left[F(t),F^\dagger(t')\right]\right\rangle = \delta(t-t'), \tag{5.11}$$

but that $\left\langle\left[F^\dagger(t'),F(t)\right]_+\right\rangle$ is not delta correlated.

In this approximation, the part of the integral in Eq. (5.1) proportional to ν will vanish, as this is an odd function, and so:

$$\begin{aligned}(\omega_0 - \mu - i\kappa)\psi_0 &= \sum_i g_i^2 \psi_0 \gamma (F_B - F_A)(\tilde{\epsilon} + i\gamma) \\ &\qquad \times \int \frac{d\nu}{2\pi} \frac{1}{[(\nu - E)^2 + \gamma^2][(\nu + E)^2 + \gamma^2]} \\ &= \sum_i g_i^2 \psi_0 (F_B - F_A) \frac{\tilde{\epsilon} + i\gamma}{4(E^2 + \gamma^2)} \end{aligned} \tag{5.12}$$

Hence, the polarisation of the two-level systems is in this case proportional to the inversion of the baths, $N_B = (n_B - n_A) = -(F_B - F_A)/2$. Using this, and taking all two-level systems to have identical energies this becomes:

$$(\omega_0 - \mu - i\kappa)\psi_0 = -N_B n g^2 \psi_0 \frac{\tilde{\epsilon} + i\gamma}{2(E^2 + \gamma^2)}. \tag{5.13}$$

This results is equivalent to that for a simple laser, as we will see next by deriving an equivalent condition from a much simpler model of pumping.

Maxwell-Bloch equations

The above result can be compared to a simple Maxwell-Bloch theory of a laser, in the semiclassical limit:

$$\partial_t \psi = -i\omega_0 \psi - \kappa\psi + gP, \tag{5.14}$$

$$\partial_t P = -2i\epsilon P - \eta P + g\psi N \tag{5.15}$$

$$\partial_t N = \lambda(N_0 - N) - 2g(\psi^* P + P^* \psi), \tag{5.16}$$

where $P = -in\langle a^\dagger b\rangle, N = n\langle b^\dagger b - a^\dagger a\rangle$, and these equations come from the Heisenberg equations of our Dicke Polariton model, with the addition of a fairly general set of decay terms. The value N_0 can be understood as a bath inversion.

The mean-field condition for a condensate $\psi = \psi_0 e^{-i\mu t}$ in this model can be written as:

$$(-i\mu + i\omega_0 + \kappa)\psi = gP \tag{5.17}$$

$$(-i\mu + 2i\epsilon + \eta)P = g\psi N, \tag{5.18}$$

which can be written as:

$$(\omega_0 - \mu - i\kappa) = -\frac{g^2 N}{2\tilde{\epsilon} - i\eta}. \tag{5.19}$$

Substituting the steady state value of P from Eq. (5.18) into Eq. (5.16) gives:

$$\begin{aligned}\lambda N_0 &= \lambda N + 2g^2 |\psi_0|^2 N \left(\frac{1}{\eta + 2i\tilde{\epsilon}} + \frac{1}{\eta - 2i\tilde{\epsilon}} \right), \\ N_0 &= N \left[1 + \frac{2g^2 |\psi_0|^2}{\lambda} \frac{2\eta}{\eta^2 + 4\tilde{\epsilon}^2} \right] \end{aligned} \tag{5.20}$$

hence we may substitute this into Eq. (5.19) to give:

$$(\omega_0 - \mu - i\kappa) = -\frac{g^2}{2\tilde{\epsilon} - i\eta} \frac{N_0(4\tilde{\epsilon}^2 + \eta^2)}{[4\tilde{\epsilon}^2 + \eta^2 + 4(\eta/\lambda)g^2|\psi_0|^2]}$$
$$= -N_0 g^2 \frac{(2\tilde{\epsilon} + i\eta)}{[4\tilde{\epsilon}^2 + \eta^2 + 4(\eta/\lambda)g^2|\psi_0|^2]} \quad (5.21)$$

Hence, if we choose $\eta = \lambda = 2\gamma$, then this is equivalent to our result in Eq. (5.13), with $N_0 \equiv nN_B$.

5.3 Generic behaviour away from extremes

Away from the extremes of laser theory or of thermal equilibrium, the effect of pumping on the phase boundary can be understood as a result of competition of two effects: Pumping and decay add noise, reducing coherence, hence suppressing condensation. On the other hand, for a given decay rate, pumping increases the density, favouring condensation. The simplest illustration of the first of these is shown in Fig. 5.2, where one sees that as the value of γ is increased, for a fixed κ, the critical density required for condensation increases. (The density may be calculated from the photon density $|\psi_0|^2$, and the fermion density $\mathrm{Tr}[G^K_{a^\dagger a} - G^K_{b^\dagger b}]$.)

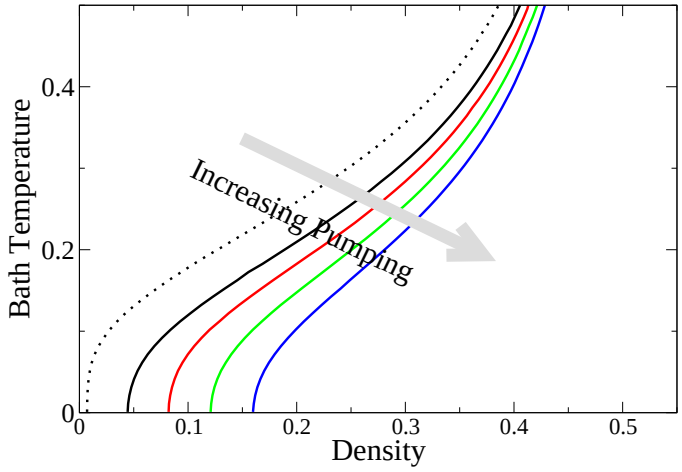

Figure 5.2: Critical temperature as a function of density, showing effects of pumping and decay.

To see the competition between pumping introducing noise and pumping overcoming decay, one may look at the low temperature limit, shown in Fig. 5.3, plotting the critical value of κ as a function of γ. Two lines are shown; the black line has an inverted bath (as would be required for the laser limit), the red line has a non-inverted bath. In the later case (as illustrated in the inset) for small γ, the two-level system energy is too far below the pumping bath and insufficiently broadened by γ to be populated.

In the presence of inhomogeneous broadening, the above picture is significantly relaxed, since the tail of the density of states can be occupied even if the peak is below the chemical potential. This is illustrated in Fig. 5.4.

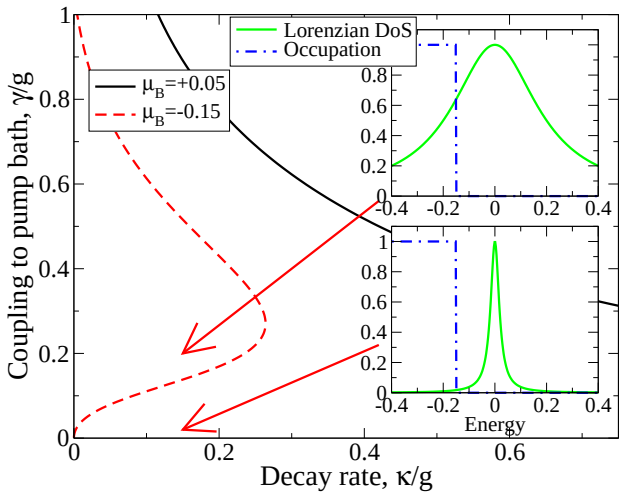

Figure 5.3: Critical couplings to pumping bath without inhomogeneous broadening and at low temperatures.

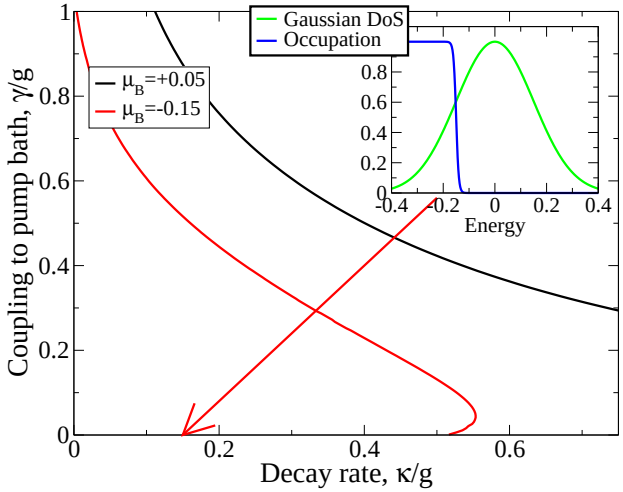

Figure 5.4: Critical couplings to pumping bath Gaussian inhomogeneous broadening ($\sigma = 0.5$) and non-zero temperature ($T = 0.1$).

Chapter 6

Fluctuations in the non-equilibrium theory

The task of this chapter is, as in chapter. 3, to determine the Green's function(s) describing fluctuations about the mean-field theory. We will first discuss the formal steps required to calculate the spectrum, and then briefly discuss what this implies for the condensed spectrum. The majority of this chapter will then discuss what can be learnt by looking at the analytic properties of the normal-state Green's function, allowing one to connect the instability of the normal state, the divergence of the occupation, and the existence of a solution to the gap equation.

6.1 Self energies and inverse photon Green's function

We will illustrate here how the Green's function can be calculated for the condensed state, but will quickly specialise to the non-condensed state. When condensed, as in Sec. 3.2 it is helpful to write the Green's function in a vector space of $\psi, \psi^\dagger$. As in the previous section, this vector space should be combined with the $\pm$ space for Keldysh and retarded/advanced Green's functions, we should write matrices in the basis $(\psi_{k,+}, \psi^\dagger_{-k,+}, \psi_{k,-}, \psi^\dagger_{-k,-})$. Unlike the fermionic case, this basis has swapped $\psi \leftrightarrow \psi^\dagger$ in some elements; this is equivalent to replacing $t \to -t$ in the time domain, so in the frequency domain, one as $\omega + i0 \to -(\omega + i0)$. Using the same approach as gave the free temperature Green's function in Eq. (3.26), we find that in our 4×4 basis we have:

$$\mathcal{D}^{-1} = \begin{pmatrix} 0 & 0 & \omega - \tilde{\omega}_k - i0 & 0 \\ 0 & 0 & 0 & -\omega - \tilde{\omega}_k + i0 \\ \omega - \tilde{\omega}_k + i0 & 0 & (2i0)F_0(\omega + \mu) & 0 \\ 0 & -\omega - \tilde{\omega}_k - i0 & 0 & (2i0)F_0(-\omega + \mu) \end{pmatrix}. \tag{6.1}$$

In this, we have written all frequencies measured relative to μ, meaning that we made the substitution $\psi_k \to e^{-i\mu t}(\psi_0 \delta_k + \psi_k)$.

In addition to the free Green's function, there are self energies due to the coupling to the decay bath and due to the coupling to the two-level systems. The former are straightforward; just as in the fermionic case we get:

$$\Sigma^{++}_{\psi^\dagger\psi}(t,t') = \sum_p \zeta^2_{p,k} D^{--}_{\Psi^\dagger\Psi} = 0$$
$$\Sigma^{-+}_{\Psi}(t,t') = \sum_p \zeta^2_{p,k} D^{+-}_{\Psi^\dagger\Psi} = -i\sum_p \zeta^2_{p,k}\theta(t-t')e^{-i\omega_p^\zeta(t-t')} = -i\kappa\delta(t-t')$$
$$\Sigma^{+-}_{\Psi}(t,t') = \sum_p \zeta^2_{p,k} D^{-+}_{\Psi^\dagger\Psi} = +i\sum_p \zeta^2_{p,k}\theta(t'-t)e^{+i\omega_p^\zeta(t-t')} = +i\kappa\delta(t-t')$$
$$\Sigma^{--}_{\Psi}(t,t') = \sum_p \zeta^2_{p,k} D^{++}_{\Psi^\dagger\Psi} = -i\sum_p \zeta^2_{p,k}[2n_\Psi(\omega_p^\zeta)+1]e^{-i\omega_p^\zeta(t-t')} = -2i\kappa\breve{F}_\Psi(t-t'),$$

In all cases, the above are expressions for the $\psi^\dagger\psi$ elements in the $\psi, \psi^\dagger$ space. The only other non-vanishing elements are the $\psi\psi^\dagger$ elements, which are related by Hermitian conjugation (in the case of Σ^R, Σ^A), or by replacing $\omega \to -\omega$ (in the case of Σ^K).

As before $\breve{F}_\Psi$ is the Fourier transform of the $2n_\Psi(\omega)+1$; these terms thus give a self energy:

$$\Sigma_\Psi = \begin{pmatrix} 0 & 0 & +i\kappa & 0 \\ 0 & 0 & 0 & -i\kappa \\ -i\kappa & 0 & -(2i\kappa)F_\Psi(\omega+\mu) & 0 \\ 0 & +i\kappa & 0 & -(2i\kappa)F_\Psi(-\omega+\mu) \end{pmatrix}. \quad (6.2)$$

When considering the self energy due to the two-level systems, we may simply the calculation by noting that only $\Sigma^R_{\psi^\dagger\psi}, \Sigma^R_{\psi^\dagger\psi^\dagger}, \Sigma^K_{\psi^\dagger\psi}, \Sigma^K_{\psi^\dagger\psi^\dagger}$ are independent; all other self energies can be related to these quantities by hermitian conjugation and/or swapping $\omega \to -\omega$. To generate these terms, the effective interaction may be written as:

$$\begin{aligned}\int_C d t \tilde{H}_{\rm int} &= \int_{-\infty}^{\infty} dt g \left[\tilde{\psi}(t,f)\tilde{b}^\dagger_i(t,f)\tilde{a}_i(t,f) - \tilde{\psi}(t,b)\tilde{b}^\dagger_i(t,b)\tilde{a}_i(t,b) + \text{H.c.}\right] \\ &= \int_{-\infty}^{\infty} dt \frac{g}{\sqrt{2}} \Big[\tilde{\psi}_+(t)\left(\tilde{b}^\dagger_{i+}(t)\tilde{a}_{i-}(t) + \tilde{b}^\dagger_{i-}(t)\tilde{a}_{i+}(t)\right) \\ &\qquad + \tilde{\psi}_-(t)\left(\tilde{b}^\dagger_{i+}(t)\tilde{a}_{i+}(t) + \tilde{b}^\dagger_{i-}(t)\tilde{a}_{i-}(t)\right) + \text{H.c.}\Big].\end{aligned} \quad (6.3)$$

(NB; the above expressions illustrate an important general feature of the interaction: each term involves an odd number of fields with the $-$ label, since the overall expression must be odd under interchanging $f \to b$ parts of the contour.)

We may now use this form of the interaction to label $\pm$ fields in the self energy diagrams; for instance, the retarded self energy (i.e. the $-+$ component) has the form:

$\Sigma^{-+}_{\rm TLS} =$ 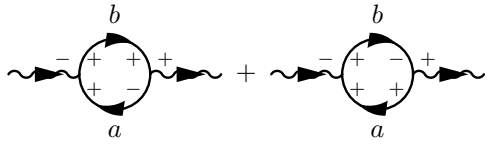

(any other set of labels will involve a $--$ line, and such Green's functions vanish). As such, we may write:

$$\Sigma^{-+}_{\rm TLS} = -i\frac{2}{2!}\left(\frac{g}{\sqrt{2}}\right)^2 \int \frac{d\nu}{2\pi} \sum_i \left[G^A_{a^\dagger a}(\nu) G^K_{b^\dagger b}(\nu+\omega) + G^K_{a^\dagger a}(\nu) G^R_{b^\dagger b}(\nu+\omega)\right]. \tag{6.4}$$

For the anomalous case, all that changes is the a, b labels, i.e.:

$$\Sigma^{-+}_{\rm TLS^\dagger} = -i\frac{2}{2!}\left(\frac{g}{\sqrt{2}}\right)^2 \int \frac{d\nu}{2\pi} \sum_i \left[G^A_{a^\dagger b}(\nu) G^K_{b^\dagger a}(\nu+\omega) + G^K_{a^\dagger b}(\nu) G^R_{b^\dagger a}(\nu+\omega)\right]. \tag{6.5}$$

The $+-$ component of Σ is just the Hermitian conjugate of the above; the $++$ component vanishes, since it either involves $--$ lines, or it involves products of two retarded Green's functions. Since the retarded Green's function is causal (i.e. it looks like $\theta(t-t')$) in the time domain, all of its poles are in the lower half plane, and so the integral of a product of two such functions is equal to zero.[1]

The only other surviving Green's function is thus:

$\Sigma^{--}_{\rm TLS} =$ 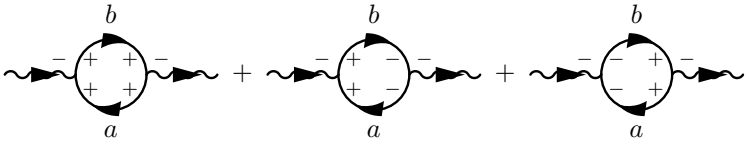

which gives the equation:

$$\Sigma^{--}_{\rm TLS} = -i\frac{2}{2!}\left(\frac{g}{\sqrt{2}}\right)^2 \int \frac{d\nu}{2\pi} \sum_i \left[G^K_{a^\dagger a}(\nu) G^K_{b^\dagger b}(\nu+\omega) + G^A_{a^\dagger a}(\nu) G^R_{b^\dagger b}(\nu+\omega) + G^R_{a^\dagger a}(\nu) G^A_{b^\dagger b}(\nu+\omega)\right]. \tag{6.6}$$

This completes the derivation of the Green's function describing fluctuations about the mean-field solution. In section 6.2, we will focus on the non-condensed spectrum, and use these results to study the instability of the normal state, and make further connections to the behaviour of a simple laser. Before this, we however first make a few comments regarding the structure of the condensed spectrum.

Comments on properties of condensed spectrum

Just as in equilibrium, the inverse Green's function can be shown to obey a Hugenholtz-Pines relation, $[D^R_{\psi^\dagger\psi}]^{-1}(0,0) = [D^R_{\psi^\dagger\psi^\dagger}]^{-1}(0,0)$, which implies

[1] NB; since the Green's function generically looks like $1/\omega$ at large ω, the integral of a single retarded Green's function depends on the regularisation used. However, for a product of retarded Green's functions, the integral is well defined, and so vanishes.

a gapless spectrum. Just as in equilibrium, one can show that this condition is equivalent to the mean-field condition we wrote previously, although the algebra here becomes rather more complicated.

It is worth noting that this statement means that the gap equation at $\psi_0 = 0$ is equivalent to the condition:

$$0 = [D^R_{\psi^\dagger\psi}]^{-1}(0,0) = \omega - \omega_0 + i\kappa - \Sigma^R_{\rm TLS}(\omega), \tag{6.7}$$

for some particular $\omega = \mu$, where we have written the non-condensed self energies without the gauge transform. (i.e., if there is no condensate, then there is no reason to gauge transform the expressions by μ.)

6.2 Discussion of non-condensed spectrum

Let us now focus on the non-condensed case, and study how the competition between the couplings to the baths sets both the spectrum and its occupation. If non-condensed, we have the simpler expression:

$$\begin{pmatrix} 0 & \omega - \omega_k - i\kappa - \left[\Sigma^R_{\rm TLS}(\omega)\right]^* \\ \omega - \omega_k + i\kappa - \Sigma^R_{\rm TLS}(\omega) & 2i\kappa F_\Psi - \Sigma^K_{\rm TLS}(\omega) \end{pmatrix} D = 0, \tag{6.8}$$

where $\Sigma_{\rm TLS}$ is the self energy due to the two-level systems given above in Eq. (6.4),(6.6), and the and the two-level system Green's functions in those equations are:

$$G^R_{b^\dagger b, a^\dagger a} = \frac{1}{\nu \mp \epsilon_i + i\gamma}, \qquad G^K_{b^\dagger b, a^\dagger a} = -\frac{2i\gamma F_{B,A}(\nu)}{(\nu \mp \epsilon_i)^2 + \gamma^2}, \tag{6.9}$$

hence we may write

$$\begin{aligned} \Sigma^R_{\rm TLS}(\omega) = -\frac{i}{2}(-2i\gamma) \int \frac{d\nu}{2\pi} \sum_i g_i^2 \\ \times \frac{(\nu + \epsilon_i + i\gamma)\, F_B(\nu+\omega) + (\nu + \omega - \epsilon_i - i\gamma)\, F_A(\nu)}{\left[(\nu+\omega-\epsilon_i)^2 + \gamma^2\right]\left[(\nu+\epsilon_i)^2 + \gamma^2\right]} \end{aligned} \tag{6.10}$$

We will later discuss the form of this function fully; for the moment, we will note only that it has an ω dependent imaginary part, and consider what physical properties depend on the form of this imaginary part. To do this, we will now discuss the analytic properties of the inverse retarded Green's function, and its connection to the spectral weight and its occupation.

Analytic properties of spectral weight and occupation

For the non-condensed case, if we write

$$\left[D^R(\omega)\right]^{-1} = A(\omega) + iB(\omega), \qquad \left[D^{-1}(\omega)\right]^K = iC(\omega),$$

then we can write the luminescent intensity, spectral weight (which becomes $-\pi\rho_L(\omega)$ in equilibrium) and occupation function in terms of these quantities and the inverse Keldysh Green's function. First, writing:

$$D^R(\omega) = \frac{A(\omega) - iB(\omega)}{A(\omega)^2 + B(\omega)^2}, \qquad D^K(\omega) = \frac{-iC(\omega)}{A(\omega)^2 + B(\omega)^2}, \tag{6.11}$$

In terms of these quantities, we may write the luminescence spectrum:

$$\begin{aligned}\mathcal{L}(\omega) &= \int \frac{dt}{2\pi} e^{i\omega t}\langle\psi^\dagger(t)\psi(0)\rangle = \frac{i}{2}\left[D^K_{\psi^\dagger\psi}(\omega) - \left(D^R_{\psi^\dagger\psi}(\omega) - D^A_{\psi^\dagger\psi}(\omega)\right)\right] \\ &= \frac{C(\omega) - 2B(\omega)}{2[A(\omega)^2 + B(\omega)^2]}\end{aligned} \tag{6.12}$$

and then, by analogy with the equilibrium system, we can explain the form of this expression in terms of a spectral weight (density of states) $\rho(\omega) = -2\Im[D^R(\omega)]$ and an occupation function $2n_\psi(\omega) + 1 = iD^K(\omega)/\rho(\omega)$, giving:

$$\rho(\omega) = \frac{2B(\omega)}{A(\omega)^2 + B(\omega)^2}, \qquad n(\omega) = \frac{1}{2}\left[\frac{C(\omega)}{2B(\omega)} - 1\right], \tag{6.13}$$

hence the luminescence is related to these as $\mathcal{L}(\omega) = \rho(\omega)n(\omega)$ as expected.

In the absence of coupling to the two-level systems, one may clearly identify the role of the three expressions involved here:

- $B(\omega) = \kappa$ is the linewidth (absorption minus gain) of the normal modes
- $A(\omega) = \omega - \omega_k$ describes the locations of these modes, and
- $C(\omega) = 2\kappa(2n_\Psi + 1)$ describes their occupation.

However, when coupled to the two-level systems, $B(\omega)$ is not a constant, hence firstly, the linewidth varies, and more importantly, $B(\omega)$ may vanish. If it does vanish then the spectral weight vanishes, and the occupation diverges, such that the luminescence remains finite.

Physically, this describes the behaviour that would, in equilibrium, be expected at the chemical potential, as long as the chemical potential lies below the bottom of the band. Furthermore, near the point where $B(\omega) = 0$, this distribution will look similar to a Bose-Einstein distribution, diverging as $1/(\omega - \mu)$. We may thus identify the effect of pumping as introducing a chemical potential that has nothing to do with the chemical potential of the decay bath. Hence, the inverse Keldysh part does not fix the distribution; it is the ratio of Keldysh and imaginary retarded Green's functions that matter. Figure 6.1 shows how the spectral weight, distribution function $2n_\psi + 1$ and luminescence are related to the zeros of the real and imaginary parts of the inverse Green's function.

Occupation at high temperatures

The above statements can be demonstrated more thoroughly in a high temperature limit, where we can approximately evaluate the integral in Eq. (6.10), and the similar expression for the Keldysh self energy. Specifically, suppose we consider $\gamma \ll T$, then the bath distribution functions do not change significantly across each Lorentzian broadened peak (but may

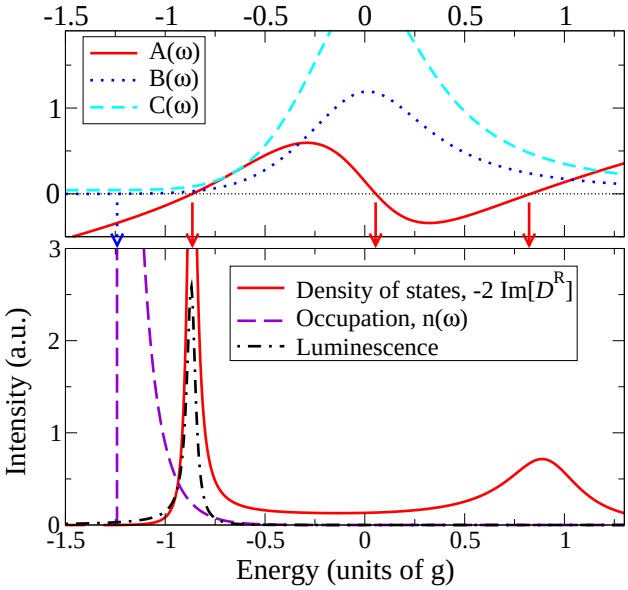

Figure 6.1: Behaviour of inverse Green's functions, and resulting properties of spectral weight, luminescence and occupation functions in the normal state. Upper panel shows the inverse Green's functions (with zeros marked by arrows), and the lower panel shows the various physical correlations of interest.

vary between the two peaks). Writing the imaginary part of the inverse Green's function, we have:

$$\begin{aligned} B(\omega) &= \kappa + \gamma^2 \int \frac{d\nu}{2\pi} \sum_i g_i^2 \frac{F_B(\nu+\omega) - F_A(\nu)}{\left[(\nu+\omega-\epsilon_i)^2+\gamma^2\right]\left[(\nu+\epsilon_i)^2+\gamma^2\right]} \\ &= \kappa + ng^2\gamma \frac{[F_B(\epsilon) - F_A(\epsilon-\omega)]}{(\omega-2\epsilon)^2+4\gamma^2}, \end{aligned} \tag{6.14}$$

where we have performed the integrals assuming the distributions are effectively constant.[2] Note that we did not yet make the same very high temperature expansion as previously, so the frequency dependence of F still persists. By using a similar approach to evaluate $[D^{-1}]^K$ we may then

[2] Formally, the above result corresponds to performing the contour integral, taking into account the poles at $\nu = -\omega + \epsilon_i + i\gamma$ and $\nu = -\epsilon + i\gamma$, but neglecting the poles from F which are at $\nu = \{-\omega + \mu_B/2, -\mu_B/2\} + i(2n+1)\pi T$, along with neglecting $\beta\gamma$ in evaluating the residues, hence:

$$\begin{aligned} I &= \int \frac{d\nu}{2\pi} \frac{F_B(\nu+\omega) - F_A(\nu)}{\left[(\nu+\omega-\epsilon)^2+\gamma^2\right]\left[(\nu+\epsilon)^2+\gamma^2\right]} \\ &= i\left[\frac{F_B(\epsilon) - F_A(\epsilon-\omega)}{(2i\gamma)(2\epsilon-\omega)(2\epsilon-\omega+2i\gamma)} + \frac{F_B(-\epsilon+\omega) - F_A(-\epsilon)}{(2i\gamma)(\omega-2\epsilon)(\omega-2\epsilon+2i\gamma)}\right] \end{aligned} \tag{6.15}$$

and then, one may make use of the symmetry $F_A(-x) = -F_B(x)$ from Eq. (5.2) to combine the remaining terms to give Eq. (6.14).

write:

$$2n_\psi(\omega)+1=\frac{\kappa(2n_\Psi(\omega)+1)+\dfrac{ng^2\gamma}{(\omega-2\epsilon)^2+4\gamma^2}(1-F_B(\epsilon)F_A(\epsilon-\omega))}{\kappa\qquad\qquad+\dfrac{ng^2\gamma}{(\omega-2\epsilon)^2+4\gamma^2}(F_B(\epsilon)-F_A(\epsilon-\omega))}. \tag{6.16}$$

This expression has a particularly simple explanation; if $\kappa \gg g^2\gamma/[(\omega-2\epsilon)^2+4\gamma^2]$, then the distribution of the photons in the cavity follows that of the decay bath. On the other hand, near resonance, the distribution is set by the pumping bath, and one has:

$$\begin{aligned}2n_\psi(\omega)+1&=\frac{1-F_B(\epsilon)F_A(\epsilon-\omega)}{F_B(\epsilon)-F_A(\epsilon-\omega)}\\&=\frac{1-\tanh\left(\frac{\beta}{2}\left[\epsilon-\frac{\mu_B}{2}\right]\right)\tanh\left(\frac{\beta}{2}\left[\epsilon-\omega+\frac{\mu_B}{2}\right]\right)}{\tanh\left(\frac{\beta}{2}\left[\epsilon-\frac{\mu_B}{2}\right]\right)-\tanh\left(\frac{\beta}{2}\left[\epsilon-\omega+\frac{\mu_B}{2}\right]\right)}\\&=\coth\left(\frac{\beta}{2}\left[\epsilon-\frac{\mu_B}{2}-\epsilon+\omega-\frac{\mu_B}{2}\right]\right),\end{aligned} \tag{6.17}$$

hence the photon distribution is exactly as expected. The results of Eq. (6.16) are shown in Fig. 6.2, with the chemical potential of the decay bath taken to be not that distant from the pumping bath. This situation is unrealistic, but is useful to illustrate the contributions to the distribution function, and to be able to show all the relevant features on a single graph.

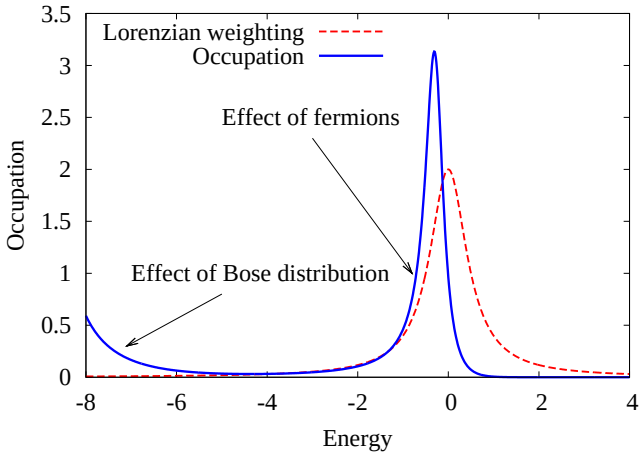

Figure 6.2: Cartoon of occupation function set by competition of bosonic bath and fermionic bath, with effect of fermionic bath moderated by a Lorentzian filter depending on excitonic energy. The chemical potential of the decay bath is at -9, and that of the pumping bath is just below zero.

Normal state instability and gap equation

Let us return to the meaning of the zeros of the real and imaginary parts of the inverse retarded Green's function. Although a zero of the imaginary

part does not cause the luminescence to diverge, a simultaneous zero of the real and imaginary parts will. Moreover, we will next show that the stability of the system depends on the ordering of the zeros of real and imaginary parts. Suppose we define $A(\omega) = \omega - \xi$, and $B(\omega) = \alpha(\omega - \mu_{\text{eff}}$ (this corresponds to focussing on the small ω region of Fig. 6.1. In this case we have:

$$\begin{aligned}[D^R]^{-1} &\simeq (\omega - \xi) + i\alpha(\omega - \mu_{\text{eff}}) \\ &= (1 + i\alpha)\left[\omega - \frac{(\xi + i\alpha\mu_{\text{eff}})(1 - i\alpha)}{1 + \alpha^2}\right], \end{aligned} \tag{6.18}$$

hence the actual poles are at frequencies:

$$\omega^* = \frac{(\xi + \alpha^2\mu_{\text{eff}}) + i\alpha(\mu_{\text{eff}} - \xi)}{1 + \alpha^2}. \tag{6.19}$$

Since these poles determine the time dependence of the retarded Green's function, we can see that if $\mu_{\text{eff}} > \xi$, then the pole has the wrong sign of imaginary part; it describes a mode the amplitude of which grows as a function of time.

Putting this together with the statement that the solution of the gap equation was equivalent to the vanishing of the inverse retarded Green's function at some frequency, we have the following scenario:

Very weak pumping For large negative μ_B, one finds that $F_B(\epsilon) - F_A(\epsilon - \omega)$ is always positive, and so no zero of $B(\omega)$ exists.

Subcritical pumping For less negative values of μ_B, there is a zero of $B(\omega)$ at μ_{eff}, so a "chemical potential" emerges, but since $\mu_{\text{eff}} < \xi_0$ the normal state is stable.

Critical pumping At some value of μ_B, one finds that $\mu_{\text{eff}} = \xi$, meaning that at this value of $\omega^* = \mu_{\text{eff}} = \xi$, one has $D^R(\omega^*) = 0$. Hence, the gap equation first has a solution at this point, there is a real divergence of the luminescence, and the normal state is marginally stable.

Supercritical pumping Above this value, the normal state would have $\mu_{\text{eff}} > \xi$, and so would be unstable.

The actual behaviour for the polariton Dicke model is shown in Fig. 6.3; one can see that a pair of zeros of the imaginary part emerge, and then one crosses the bottom of the polariton modes. Note that in equilibrium, we have $\mu_{\text{eff}} = \mu = \mu_B$ at all conditions, and the so only the last three stages of the above scenario exist; condensation occurs when the chemical potential reaches the bottom of the band.

Comparison to Maxwell-Bloch equations

It is instructive to compare the above scenario to that for a simple laser in the Maxwell Bloch equations. We may find the retarded Green's function

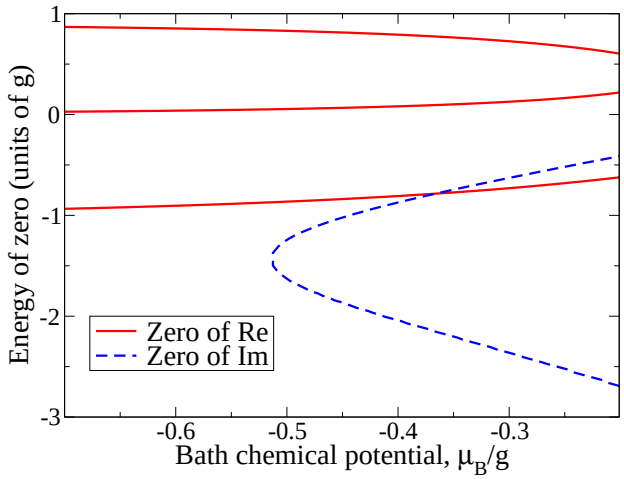

Figure 6.3: Variation of energies of zeros of real part of inverse Green's function and imaginary part as density is varied via chemical potential of pumping bath

by the response to an applied force $F = e^{-i\omega t}$ acting on the photons, in the absence of a laser field. In this limit Eq. (5.16) becomes $N = N_0$ and taking $\eta = 2\gamma$ as we found previously Eq. (5.14)– (5.15) become:

$$\partial_t \psi = -i\omega_0 \psi - \kappa\psi + gP + Fe^{-i\omega t}$$
$$\partial_t P = -2i\epsilon P - 2\gamma P + g\psi N_0,$$

hence if $\psi = iD^R(\omega)Fe^{-i\omega t}, P = \chi(\omega)\psi$, we have:

$$(-i\omega + i\omega_0 + \kappa - g\chi)iD^R = 1$$
$$(-i\omega + 2i\epsilon + 2\gamma)\chi = gN_0,$$

allowing us to write:

$$[D^R]^{-1} = \omega - \omega_0 + i\kappa + \frac{g^2 N_0}{\omega - 2\epsilon + i2\gamma}. \tag{6.20}$$

Alternatively, we may return to Eq. (6.10) when F_B, F_A are constants and write:

$$\Sigma^R_{\rm TLS}(\omega) = -\sum_i \int \frac{d\nu}{2\pi} \left[\frac{g_i^2 \gamma F_B}{(\nu + \epsilon_i - i\gamma)\left[(\nu + \omega - \epsilon_i)^2 + \gamma^2\right]} \right.$$
$$\left. + \frac{g_i^2 \gamma F_A}{(\nu + \omega - \epsilon_i + i\gamma)\left[(\nu + \epsilon_i)^2 + \gamma^2\right]} \right]$$
$$= -\sum_i \frac{g^2}{2} \frac{F_A - F_B}{\omega - 2\epsilon + 2i\gamma}, \tag{6.21}$$

and so, identifying the bath inversion $N_B = (F_A - F_B)/2$ we may write:

$$[D^R]^{-1} = \omega - \omega_0 + i\kappa + \frac{g^2 n N_B}{\omega - 2\epsilon + 2i\gamma}, \tag{6.22}$$

and we can again identify the total bath inversion $N_0 = nN_B$.

In either case, we may notice a number of features; firstly, for there to be a zero of the imaginary part, we require:

$$0 = \kappa[(\mu_{\text{eff}} - 2\epsilon)^2 + 4\gamma^2] - 2\gamma g^2 N_0, \quad \mu_{\text{eff}} = 2\epsilon \pm \sqrt{g^2 N_0 \frac{2\gamma}{\kappa} - 4\gamma^2}. \quad (6.23)$$

Clearly, this only has solutions if $N_0 > 0$ (and in fact is more restrictive, requiring $g^2 N_0 > 2\gamma\kappa$). In the special case of zero detuning, $\omega_0 = 2\epsilon$, we can also find the zeros of the cubic equation that is the real part:

$$0 = (\omega - 2\epsilon)\left[(\mu_{\text{eff}} - 2\epsilon)^2 + 4\gamma^2\right] + g^2 N_0\big] \quad (6.24)$$

which has the solutions:

$$\omega = 2\epsilon, \quad 2\epsilon \pm \sqrt{-4\gamma^2 - g^2 N_0}. \quad (6.25)$$

Hence, the strongly coupled modes only exist for $g^2 N_0 < -4\gamma^2$, and so the instability of the normal state only occurs after the normal mode has collapsed. This is illustrated in Fig. 6.4.

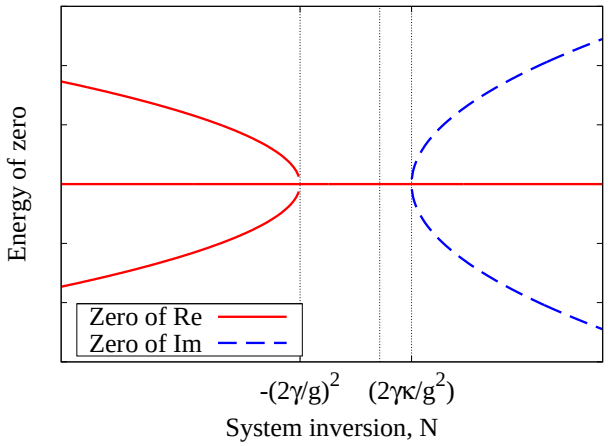

Figure 6.4: As for Fig. 6.3 but for the results of the Maxwell-Bloch equations, showing the rather different behaviour in the extreme laser limit

Bibliography

[1] J. Keeling, P. R. Eastham, M. H. Szymanska, and P. B. Littlewood, Phys. Rev. B **72**, 115320 (2005), DOI: 10.1103/PhysRevB.72.115320.

[2] M. H. Szymańska, J. Keeling, and P. B. Littlewood, Phys. Rev. B **75**, 195331 (2007), DOI: 10.1103/PhysRevB.75.195331.

[3] J. Keeling, F. M. Marchetti, M. H. Szymańska, and P. B. Littlewood, Semicond. Sci. Technol. **22**, R1 (2007), DOI: 10.1088/0268-1242/22/5/R01.

[4] J. Keeling, M. H. Szymanska, and P. B. Littlewood, in Optical Generation and Control of Quantum Coherence in Semiconductor Nanostructures, edited by G.Slavcheva and P. Roussignol (Springer, 2010).

[5] L. P. Pitaevskii and S. Stringari, Bose-Einstein Condensation (Clarendon Press, Oxford, 2003).

[6] A. Griffin, D. W. Snoke, and S. Stringari, eds., Bose-Einstein Condensation (Cambridge University Press, Cambridge, 1995).

[7] P. B. Littlewood, P. R. Eastham, J. M. J. Keeling, F. M. Marchetti, B. D. Simons, and M. H. Szymanska, J. Phys.: Condens. Matter **16**, S3597 (2004), DOI: 10.1088/0953-8984/16/35/003.

[8] A. Abrikosov, L. Gorkov, and I. Dzyaloshinski, Methods of Quantum Field Theory in Statistical Physics (Dover, New York, 1975).

[9] L. V. Keldysh, JETP **20**, 1018 (1965).

[10] E. M. Lifshitz and L. P. Pitaevskii, Physical Kinetics (Butterworth-Heinemann, Oxford, 1999).

[11] A. Kamenev, in Nanophysics: Coherence and transport, edited by H. Bouchiat, Y. Gefen, S. Guéron, G. Montambaux, and J. Dalibard (Elsevier, Amsterdam, 2005), vol. LXXXI of Les Houches, p. 177.

[12] M. O. Scully and M. S. Zubairy, Quantum Optics (Cambridge University Press, 1997).

[13] O. Penrose and L. Onsager, Phys. Rev. **104**, 576 (1956).

[14] L. V. Keldysh and A. N. Kozlov, Sov. Phys. JETP **27**, 521 (1968).

[15] C. Comte and P. Nozières, J. Physique **43**, 1069 (1982).

[16] V. N. Popov, Functional Integrals in Quantum Field Theory and Statistical Physics (D. Reidel, Dordrecht, 1983).